TALLINNA TEHNIKAÜLIKOOL
TALLINN UNIVERSITY OF TECHNOLOGY

Department of Materials and Environmental Technology

STUDY OF PHOTOCATALYTIC ACTIVITY OF THIN FILMS FOR AIR PURIFICATION

ÕHUKESTE KILEDE FOTOKATALÜÜTILISE AKTIIVSUSE UURIMINE ÕHU PUHASTAMISEL

MASTER THESIS

Student Angelina Prokofjeva
/name/

Student code KAKM153576

Supervisor Marina Kritševskaja
/name/

Tallinn, 2017

AUTHOR'S DECLARATION

Hereby I declare, that I have written this thesis independently.
No academic degree has been applied for based on this material.
All works, major viewpoints and data of the other authors used in this thesis have been referenced.

"....." ..... 201…..

Author: .....
/signature /

Thesis is in accordance with terms and requirements

"....." ..... 201….

Supervisor: ….....
/signature/

Accepted for defence

"....."....."....201… .

Chairman of theses defence commission:
.....
/name and signature/

Table of Contents

List of abbreviations

CA	cellulose acetate
CB	conduction band
eV	electron volt
FESEM	field emission scanning electron microscopy
FTIR	Fourier-transform infrared spectroscopy
GAC	granular activated carbon
HVAC	heating, ventilation and air conditioning
IR	infrared
MTBE	methyl tert-butyl ether
PAH	polyaromatic hydrocarbons
PCB	polychlorinated biphenyl
PDMS	polydimethylsiloxane
PEG	polyethylene glycol
PM	particulate matter
POP	persistent organic pollutant
ppm	parts per million
ppmv	parts per million by volume
PPO	polyphenylene oxide
PSF	polysulfone
SA	stearic acid
SEM	scanning electron microscopy
SNMS	secondary neutral mass spectrometry
TBF	tert-Butyl formate
TBOT	tetrabutyl orthotitanate
TEOS	tetraethyl orthosilicate
UV	ultraviolet
UV-VIS	ultraviolet–visible
VB	valence band
VOC	volatile organic compound
WHO	World Health Organization
XRD	X-ray diffraction

Introduction

Today, due to urbanization, half of the world's population lives in cities. Because of the rapid growth of urban areas, industrial progress and heavy traffic increase, outdoor air quality is dramatically worsening. A lot of non-toxic and toxic chemical compounds are emitted into the atmosphere by vehicles, chemical and agricultural industries. It is essential to measure the concentrations of prevailing pollutants in the air. Particulates, ozone, nitrogen and sulfur gases, carbon monoxide, volatile organic compounds (VOCs), heavy metals, polycyclic aromatic hydrocarbons (PAHs), tobacco smoke and bioaerosols are responsible for the adverse effects on human health. According to the World Health Organization (WHO) statistics, global deaths from air pollution in 2012 were about 7 million, of which 4.3 million deaths were attributable to household air pollution and 3.7 million to outdoors air pollution, of which 1 million to a combination of these two. Urban air pollution components, especially VOCs, lead to sensory irritation in eyes and airways (Jones 1999; Curtis et al. 2006; Block et al. 2012; WHO 2014).

Many different methods are being applied and developed in order to deal with air, water and soil pollution. These technologies are aiming to remove or degrade harmful chemical substances. One of the methods, which is already being studied since 1920s and was applied to pollution clean-up for the first time in 1970s, is TiO_2 photocatalysis (Hashimoto et al. 2005). It has demonstrated its power by successfully removing VOCs from different environments. Main advantages and disadvantages of this technique are addressed in this thesis. The phenomenon of photocatalytic oxidation requires a photocatalyst, which accelerates the reaction of pollutant removal, and a source of irradiation, usually ultraviolet (UV) light. The main goal of engineers and scientists is to determine the optimal design of photocatalytic composite materials, air and water purification systems, and the operating conditions which would allow for the fast and maximum degradation of pollutants (Huang et al. 2016).

The objective of this thesis is to investigate and report on the photocatalytic activity of the catalyst film under different operating conditions. The catalyst used in the study is the thin titania film prepared by sol-gel method from tetrabutyl orthotitanate (TBOT) used as precursor with the addition of stearic acid. The film is attached to the soda-lime glass plates. The conditions which were varied during the study are the methyl tert-butyl ether (MTBE) (pollutant) inlet concentration, its specific residence time, irradiation source and relative humidity of polluted air. The results will be presented and analyzed in the experimental part of the thesis. Theoretical basics are covered in

the literature review, and they focus on the phenomena of photocatalysis, gas-phase photocatalysis in particular, photocatalytic coatings, air pollutants and other air purification methods.

1 Literature review

1.1 Adverse effects of polluted air

Air pollution is believed to be associated with a wide array of health abnormalities and issues. Components of air pollution affect respiratory, cardiovascular, reproductive and central nervous systems. Elevated air pollution can result in decreased cognitive function, worsening of childhood asthma and increased risk of infection and lung cancer. Evidence suggests that long-term exposure to pollutants may be considered a risk factor for Alzheimer's and Parkinson's diseases. Some groups of people may be even more sensitive to outdoor pollutants in particular. The culprits of polluted outdoor air are mainly of anthropological origin, such as traffic, coal fired power plants, burning of biomass fuels and industrial pollution. Beijing, Shanghai, Bombay, Karachi, Cairo, Sao Paulo and Mexico City are the cities with the most problematic air conditions in the developing world (Curtis et al. 2006; Power et al. 2011; Block et al. 2012; Chin-Chan et al. 2015). Moreover, high levels of primary particulate matter emissions and secondary aerosol precursors, including SO_2, NO_x and especially VOCs, lead to heavy haze formation, thus impairing visibility (Huang et al. 2014).

Dangerous substances could be present both outdoors and indoors. Some substances may in certain cases reach even higher concentrations indoors than outdoors (Sofuoglu et al. 2010). Some VOCs, including formaldehyde, which may be present in occupational settings, can lead to sensory irritation. However, concentrations of VOCs are usually too low in dwellings and office buildings, and they do not cause sensory irritation. Asthmatics and elderly people may be more sensitive to certain indoor substances than other population groups. Even though VOC levels may be low, they could impact perceived, or subjective, sensory irritation, especially in the environments with inadequate relative humidity levels. One of the VOCs, formaldehyde, is a matter of concern because it is carcinogenic and universally present (Wolkoff 2013).

Air pollution damages not only human health, but it also negatively impacts ecosystems and building materials (through the effects of acid rain and fungal growth). Cultural heritage sites and buildings could be susceptible to erosion and degradation because of the impact of anthropogenic sources like combustion (Graue et al. 2013). The effects of pollution also include soil and aquatic acidification, N enrichment and accumulation in living organisms. Crop yield and sensitive plant species could also be affected by air pollutants. Most ecosystem types are affected by multiple air pollutants (Lovett et al. 2009; Greaver et al. 2012).

1.2 Air pollutants

Air pollution is a complex mixture of various substances. The main source of their origin is anthropogenic – combustion of fossil fuels. These chemicals could be grouped into several classes: particulate matter, persistent organic pollutants (POPs), heavy metals and gaseous pollutants (Curtis et al. 2006).

1.2.1 Particulate matter

Particulates is the large range of solid or liquid organic and inorganic particles in the air, such as metals, PAHs, dioxins and organic components. The sources of particulate matter pollution are factories, power plants, diesel exhaust, construction activity, biomass burning, volcanic ash, bioaerosols and dust from soil and roads. Particulates which are especially toxic are PM_{10} and $PM_{2.5}$ because of their size (10 micrometers and 2.5 micrometers respectively). These particles are small enough to penetrate the lung alveoli. Toxic effects largely depend on size, chemical composition and surface of particles (Curtis et al. 2006; Kampa & Castanas 2008).

1.2.2 Persistent organic pollutants (POPs)

Persistent organic pollutants are mainly aromatic hydrocarbons containing Cl which are resistant to environmental degradation. These may be carcinogenic compounds which lead to gene damage. They bioaccumulate in fatty tissues of biological organisms due to their lipophilic properties. Their concentration, and, consequently, toxicity, increases at successively higher levels in a food chain (bioamplification). They could be found everywhere in the environment - in biota, soil, water and particularly in air. They are released into air during the improper use and/or disposal of agrochemicals and industrial chemicals and due to combustion processes. Persistent organic pollutants include pesticides, dioxins, furans and PCBs (Curtis et al. 2006; Kampa & Castanas 2008; UN Environment 2014).

1.2.3 Heavy metals

Most heavy metals, such as cadmium, chromium, lead, manganese, mercury, nickel, silver and vanadium, are posing a threat to the environment and humans. For example, it was shown in a study from Taiwan that IQ of children who had high lead blood levels was lower than IQ of unexposed children (Wang et al. 1998). Heavy metals bio-accumulate in living organisms. Typically, they could be present in air and water bodies as pollutants. Known sources of heavy

metal pollution are industrial and manufacturing facilities, coal burning, metal mining, smelting, combustion, waste water and volcanic emissions (Curtis et al. 2006; Kampa & Castanas 2008).

1.2.4 Gaseous pollutants (CO, NOx, O_3, SO_2, VOCs)

Gaseous pollutants are another important class of air pollutants.

Carbon monoxide (CO) is a colorless, odorless and tasteless gas, which primarily originates from vehicles as a product of incomplete combustion. Other sources are heating, coal-fired power generation and biomass burning (Curtis et al. 2006).

Nitrogen oxides are also emitted during various combustion processes or during the oxidation of nitrogen fertilizers (Curtis et al. 2006). One study showed that if outdoor concentrations of carbon monoxide and nitrogen oxides are high, then they lead to the increased incidence of headache attacks in people who are prone to them (Nattero & Enrico 1996). Another study suggested that high levels of particulate matter and NO_2 in Shanghai were associated with death rates from stroke (Kan et al. 2003).

Another gaseous chemical, *ozone (O_3)*, is generated as a result of a cascade of different atmospheric reactions which involve VOCs, NO_x and the energy of sunlight. Lightning also produces ozone molecules. The tropospheric O_3 is a harmful pollutant, while O_3, which is the composite of the ozone layer in the stratosphere, forms a shield which protects the planet from the damaging UV (Brook et al. 2002). It was suggested that ozone and aeroallergens might work synergistically and cause severe asthma morbidity (Dales et al. 2004).

Sulfur dioxide (SO_2) is a toxic gas with a pungent smell, which is produced by burning of sulfur-containing fossil fuels, smelting of sulfur-containing ores, vehicle emissions and volcanoes. Sulfur dioxide and mercaptans are emitted during papermaking, rayon manufacturing, from coke ovens and other industries (Curtis et al. 2006). Even relatively low concentrations of outdoor SO_2 and CO can influence birth outcomes and increase the risk of preterm births, which was shown in a study conducted in Canada (Liu et al. 2003).

A lot of attention has drawn a special class of gaseous pollutants – *volatile organic compounds (VOCs)*. Volatile organic compounds are organic compounds which have high vapor pressure at room temperature. They are easily evaporated into the atmosphere. This group is composed of a large amount of low molecular weight pollutants. They include such compounds like aldehydes, ketones, esters, terpenes, alkanes, alkenes, aromatic-, fatty-, halogenated- and oxygenated-hydrocarbons (Li et al. 2009; Huang et al. 2016). More than one hundred VOCs were qualitatively

identified indoors. VOCs which could be detected indoors are usually aldehydes, ketones, alcohols (or alkoxyalcohols) and aromatics (Mo et al. 2009).

Prominent sources of VOCs are petroleum refining, petrochemicals, automobile exhaust, natural gas fields and distribution lines, storage of fuels and wastes, household products, pesticides, fuel combustion, industrial discharges, food barbecue and volatile emissions from coniferous forests. Among those, automobile exhaust is the major pollution source in cities. Alkanes, alkenes and such aromatic compounds like benzene and toluene play an important role in formation of photochemical smog and generation of formaldehyde and other reactive compounds (Curtis et al. 2006; Kampa & Castanas 2008; Huang et al. 2016).

Interestingly, some VOCs levels indoors may be up to 5 times higher than those of outdoors (US EPA 2016). Some VOCs are linked to the sick building syndrome. They are easily absorbed through skin and across mucous membranes (Brinke et al. 1998). Data from one study suggested that exposure to VOCs, including emissions from chemical manufacturing plants, is associated with increased rates of doctor-diagnosed asthma in children (Ware et al. 1993). VOCs are widely used in production of refrigerants, plastics, adhesives, paints and petroleum products (Zogorski et al. 2001).

Present study will focus on the photocatalytic oxidation of the representative of VOCs — methyl tert-butyl ether (MTBE). Therefore, properties and health effects of this chemical are given in more detail hereafter.

Methyl tert-butyl ether

The molecular formula of MTBE is $(CH_3)_3COCH_3$ (Fig. 1). It is a colorless liquid with a distinctive anesthetic-like odor. Vapors are heavier than air, and they are narcotic. MTBE can be easily produced, and is inexpensive. Nearly all MTBE produced in the United States is used as an additive in unleaded gasoline to increase octane levels. It was used in the past to produce isobutene (NCBI 2005). MTBE is a gasoline oxygenate, which adds oxygen in order to decrease vehicular CO emissions and O_3 levels in the atmosphere. MTBE has the highest production volume of all fuel oxygenates, with a worldwide production capacity of around 25 million tons (Zogorski et al. 2001; François et al. 2002). MTBE is resistant to natural degradation because of the ether bond and branches in its structure (François et al. 2002).

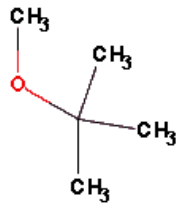

Figure 1. MTBE chemical structure, ether bond (red)

MTBE is not only an air pollutant, but also a persistent groundwater and surface water pollutant. It has high water solubility, low soil adsorption coefficient, low Henry coefficient and very low taste and odor threshold in water (Table 1). The half-life of MTBE in the air may be as short as 3 days. Several methods exist which can remove MTBE from air. These include adsorption, biofilter, thermal treatment, membrane and advanced oxidation. If air is not highly contaminated, then two first technologies are commonly applied (Mohammad et al. 2013).

Table 1. Properties of methyl tert-butyl ether (US EPA 2004)*

Molecular formula	$C_5H_{12}O$
Molecular weight	88.2 g mol^{-1}
Density	740 kg m^{-3}
Melting point	−109 °C
Boiling point	55.2 °C
Henry's law constant	0.018 at 20 °C
Odor threshold	0.053 ppm
Taste threshold in water	20-40 mg L^{-1}
Solubility in water	43,000-54,300 mg L^{-1}
Vapor pressure	245-256 mm Hg
Octane number	110

* Respective data are given for T = 25 °C, P = 100 kPa unless otherwise specified

According to the National Institute for Occupational Safety and Health, MTBE can be absorbed into the body by inhalation and by ingestion. Inhalation can cause drowsiness, dizziness, headaches, weakness and unconsciousness. Ingestion causes the abdominal pain, nausea and vomiting. Skin irritation or dryness may occur if MTBE comes into contact with skin (NIOSH 2015).

Scientists have been interested in health effects of MTBE which is emitted into the atmosphere in the form of vehicle exhaust. Some studies have found the correlation between high levels of MTBE in the air and the incidents of asthma and wheezing (difficulty to breathe) (Joseph & Weiner 2002). To the contrary, other studies have not found any increase in claims for respiratory illness after introduction of MTBE into gasoline (Gordian et al. 1995).

1.2.5 Bioaerosols

Other types of air pollutants could be grouped under the bioaerosols category. Bioaerosol sources include living organisms (mainly pathogens) and their products of metabolism. Typical examples are molds, fungi, algae, protozoa, bacteria, pollen, seeds, spores and others. These bioaerosols can be toxic and allergenic.

1.2.6 Radiation

Another type of pollution is radiation. The main sources include nuclear explosions and detonations of nuclear weapons, nuclear accidents, mining of radioactive ores, nuclear waste and nuclear medicine facilities. Effects of radiation are being studied throughout the world. One such study examined children, who had suffered prenatal radiation exposure at the time of the Chernobyl accident in 1986. They found that these children were more likely to be psychologically impaired, had specific developmental speech-language disorders and their mean IQ was lower in comparison with the control group (Kolominsky et al. 1999; Curtis et al. 2006; Environmental Pollution Centers 2017).

All in all, combinations of different types or classes of air pollutants may have a synergistic and even more adverse effect on human health and the environment than just one single pollutant.

1.3 Methods of air purification

It is evident that air pollution causes millions to suffer from different serious illnesses or experience discomfort and some health issues. In 2013, it was estimated that reducing urban air pollution would lead to huge health and monetary gains. In Europe, the monetary gain could total €31 billion per year, including savings on health expenditures, absenteeism and intangible costs such as well-being, life expectancy and quality of life. It is absolutely crucial that the urban air is not a threat to the health of Europe's population and is not a burden on European economy (Pascal et al. 2013). The prevention of outdoor pollution includes alternative fuels, improved sanitation, efficiencies and industrial processes. In order to improve indoor quality, several aspects need to be taken into

consideration - emission source control, ventilation and air cleaning. The most popular technologies for air purification will be discussed in the present segment.

In the method of *thermal treatment*, vapor-phase contaminants are degraded via high-temperature oxidation. Thermal oxidation and catalytic oxidation are the types of thermal treatment technology. Thermal oxidation employs flame to create quite high temperatures which are needed for contaminant oxidation. It is used when MTBE concentrations are 2,000 parts per million by volume (ppmv). The advantage of this method is that it makes the removal of high quantity of a contaminant possible, it does not produce secondary pollution and is highly efficient. However, it is expensive because it needs high input of energy. Dust particles and droplets are not allowed in gas which is being purified. During catalytic oxidation, lower temperatures are used because of the presence of a catalyst (e.g. Pt, Pd). VOC concentrations should be between 100 and 2,000 ppmv. The products are mostly CO_2 and H_2O (US EPA 2004).

The next technology is *biofilters*. A fixed-film bioreactor is used, in which pollutants can be biodegraded by various kinds of microorganisms. Low efficiencies are the main drawback of the method. Biofilters are usually utilized in pilot-scale studies and experimental trials. The equipment is usually big and long residence times are needed. They are suitable for low pollutant concentrations and do not harm the environment. In addition, low energy consumption is required to make this process work (US EPA 2004). For example, a thermophilic biofilter was tested for the removal of MTBE from the waste air stream. Bed temperature in all experiments was 52 ± 3 °C. It was shown that biofilter could effectively remove MTBE, with efficiencies reaching 99%. It is clear that more studies are needed to be done in order to refine biofilters and to find optimal conditions for their application (Moussavi et al. 2009).

Indoor VOCs could be also removed using the method of *botanical purification*. Pollutants come into contact with planted plants and a planted soil. Microorganisms or plants then degrade the chemicals. By-products of this technique are CO_2, organic and aminoacids. The advantages of this method are low cost and the lack of secondary pollution. Yet botanical purification is not effective for high levels of contaminants (Soreanu et al. 2013).

The other technique is a *membrane catalytic reactor*. It is a unit which includes a membrane and a reactor. Chemical reaction and separation by affinity take place simultaneously in a membrane catalytic reactor. The process is simple, energy-efficient and does not produce secondary emissions. However, this method is costly and needs more research. Different membranes and process conditions are being studied to determine which ones are more effective for pollutants,

including MTBE, removal. For example, polyphenylene oxide (PPO), polysulfone (PSF) or cellulose acetate (CA) membranes are being studied. Membranes can get exhausted and unstable (Choi et al. 2000).

The next method is physical *adsorption*, which is the most traditional method for VOCs removal. Pollutants are adsorbed onto a large-surface medium, such as granular activated carbon (GAC), activated alumina, zeolites or resin, by Van der Waals or forming new chemical bonds. Adsorption transfers the toxins to another phase rather than eliminating them altogether. The removal performance typically depends on adsorbent properties. The advantage of adsorption is the ability to remove low concentrations of a pollutant. VOC concentrations should be between 35 and 100 ppmv. The process happens at room conditions. One disadvantage is that adsorbents can have low stability and they get spent. In case of zeolites, pollutant reemission can occur. Post-treatment of adsorbent is needed. Treated pollutants usually include gases, fumes and odors (US EPA 2004; Huang et al. 2016).

Chemical *absorption* helps to remove VOCs, such as formaldehyde, from gas streams via liquid solvents. Soluble VOCs are transferred into the liquid phase. VOCs concentration should be from 500 to 5,000 ppm. VOC removal efficiencies may reach up to 95-98%. The drawback is that contaminated water is produced. It is a complex process and quite often costly (Khan & Kr. Ghoshal 2000).

Some VOCs, smells, gases and microorganisms can be eliminated from air via *ozonation*. UV or non-thermal plasma discharge generate O_3 molecules. They react with pollutants and oxidize them. O_3 may produce $OH^{\bullet}$ radicals. O_3 levels need to be strictly under control. Humidity level, contaminant types and retention time influence the final result of the process (Zhong & Haghighat 2015).

VOCs including MTBE could be degraded using *UV-photocatalytic oxidation*, developed since 1972. It is environmentally friendly, highly-chemical stable, inexpensive technique, energy-efficient and effective in removing various environmental pollutants. It degrades toxic chemicals into final benign products (CO_2 and H_2O). However, an UV source is needed. During the process, contaminants are degraded on a photocatalyst surface in the presence of light. Photocatalytic oxidation operates at room temperature and pressure. Unfortunately, intermediates can form if degradation process is not complete (Lim et al. 2009; Huang et al. 2016). The most popular photocatalyst is TiO_2 because it is non-toxic, has high photocorrosion resistance and not expensive (Schneider et al. 2014). TiO_2 could be added to different building materials, such as roofing tiles,

corrugated sheets, asphalt, pavement and walls in order to remove VOCs directly from the outdoors air and to battle urban pollution (Demeestere et al. 2008). Some disadvantages also include an UV lamp replacement, a photocatalyst deactivation and the need of its regeneration or replacement. Treated pollutants include VOCs, microbes, soot, inorganic chemicals. Factors which affect photocatalytic oxidation are humidity, light source, intensity, pollutant concentration, photocatalyst type, purification system design (Zhong & Haghighat 2015).

In conclusion, many methods are still not studied thoroughly enough and not widely used in practical applications yet. The fact that air pollution consists of many pollutants of different nature and not of only one chemical should be taken into account. Conditions and environmental processes could also determine outcomes and efficiencies of air purification systems. For instance, combinations of different methods could be applied into one hybrid cleaning system in order to boost the removal efficiency. It is unlikely that photocatalytic oxidation can effectively eliminate particulate matter. Therefore, using electrostatic precipitation to remove particulates and photocatalytic oxidation to degrade VOCs together could be more powerful. Energy consumption also determines the prospects of using one method over another (Huang et al. 2016).

1.4 Fundamentals of photocatalytic oxidation

Photocatalytic oxidation (Greek ‘phos’, ‘photos’ – light) is a phenomenon in which a photocatalyst harnesses the energy of light in order to accelerate the oxidation of a substance (Fig. 2). Nano-semiconductor catalyst reduces the activation energy of the whole degradation process and is not typically consumed in the end. The most popular photocatalyst is TiO_2. It has the most efficient photoactivity and the highest stability. It is inexpensive, and has been used as a white pigment from ancient times, and thus, environmentally friendly and non-toxic to human health. Other photocatalysts include CeO_2, SnO_2, Fe_2O_3, WO_3, ZnO, ZnS, ZrO_2 and many others. The common light source required is UV lamps (Hashimoto et al. 2005; Mamaghani et al. 2017).

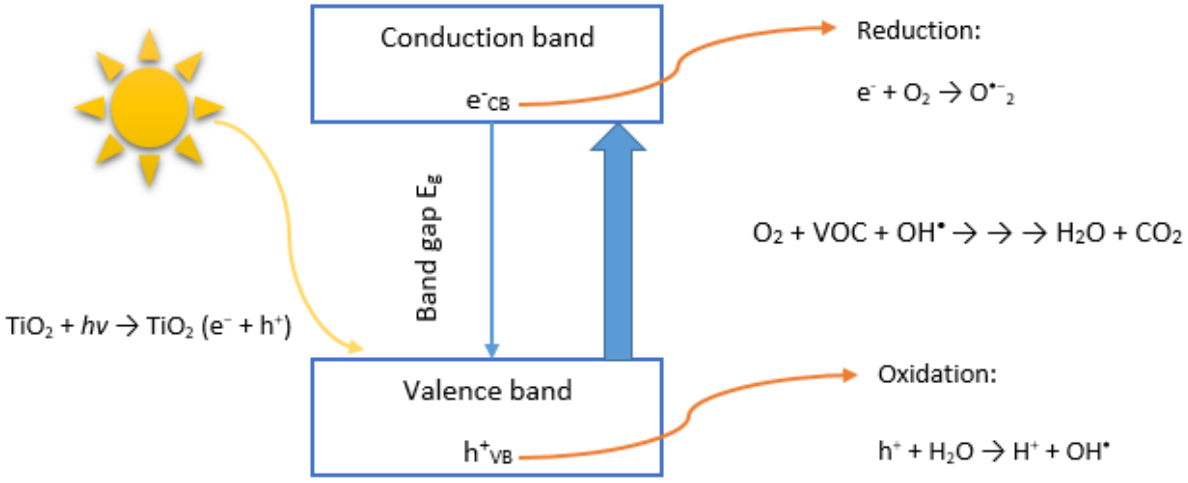

Figure 2. Schematic illustration of TiO_2 UV photocatalytic oxidation (modified from Banerjee et al. 2015)

The whole process starts with the UV light exciting a photocatalyst's *electron (e^-)* in an electron-filled valence band (VB). Energy of a photon has to be greater than or equivalent to the band gap energy of TiO_2 so that an electron could be transitioned to a vacant conduction band (CB). The UV light is the provided energy source, but it accounts only for 5% of the solar energy. The wavelength between 300-365 nm provides enough energy to overcome the band gap of TiO_2 (3.2 eV). The valence band is then left with a *positive hole (h^+)*. After that, electrons take part in reduction reactions, and positive holes in oxidation reactions of oxygen and water (Table 2, Reactions 1-10).

Table 2. Reactions involved during photocatalytic oxidation (Ren et al. 2017)

Description	**Reaction**	
Activation of photocatalyst	$TiO_2 + hv \rightarrow TiO_2 (e^- + h^+)$	(1)
Reduction of oxygen	$e^- + O_2 \rightarrow O^{\bullet-}_2$ (superoxide radical)	(2)
Oxidation of water or hydroxide ion	$h^+ + H_2O \rightarrow H^+ + OH^\bullet$	(3)
	$h^+ + OH^- \rightarrow OH^\bullet$	(4)
Hydroperoxyl radical formation	$O^{\bullet-}_2 + H^+ \rightarrow HO_2^\bullet$	(5)
Hydrogen peroxide formation	$2HO_2^\bullet \rightarrow O_2 + H_2O_2$	(6)
	$HO_2^\bullet + e^- + H_2O \rightarrow H_2O_2 + OH^-$	(7)
	$2\ OH^\bullet \rightarrow H_2O_2$	(8)
Hydroxyl formation from peroxide	$H_2O_2 + e^- \rightarrow OH^\bullet + OH^-$	(9)
Reaction with VOC	$O_2 + VOC + OH^\bullet \rightarrow H_2O + CO_2 +$ other products	(10)

The produced hydroxyl radical ($OH^{\bullet}$) is a strong oxidant. In the presence of oxygen, it attacks pollutants, e.g. VOCs, which get adsorbed onto the surface of a photocatalyst (Mo et al. 2009; Huang et al. 2016).

Alternatively, electrons and positive holes, with a lifetime of nanoseconds, can undergo the recombination process, where they neutralize each other. This negatively affects the performance of photocatalytic oxidation (Wen et al. 2015). Oxidation series of VOCs usually consists of more than one elementary step. Theoretically, it is possible to completely degrade VOCs into H_2O and CO_2 (complete mineralization). However, given the short residence time and inadequate adsorption, the reaction often stops with the formation of intermediates (sometimes also called 'by-products'). Among these intermediates – aldehydes, ketones or organic acids. It is the main disadvantage of the photocatalytic oxidation process because these intermediates may be even more damaging to human health and the environment than initial compounds. This fact should be taken into consideration when implementing any air purifying system based on photocatalytic oxidation into a building. Intermediates can also deactivate a photocatalyst (Mo et al. 2009).

1.5 Gas-phase photocatalysis

In order to apply photocatalytic oxidation for air purification, some aspects should be taken into account. First of all, a photocatalyst should possess the adequate photocatalytic activity and physicochemical stability. The common photocatalyst is anatase TiO_2. Secondly, air purification systems should be designed properly. Thirdly, various conditions and their effects on photocatalysis need thorough examination. It is also crucial that any produced intermediates of pollutants are not toxic and/or completely oxidized into non-harmful substances (Ren et al. 2017).

The first step during the gas-phase photocatalytic oxidation is the advection of the pollutants in the air flow. Gas-phase photocatalytic oxidation also involves mass transfer of the contaminants from the gas phase to the solid phase. It affects the reaction rate and removal efficiency. Pollutants diffuse from bulk to exterior surface and after that diffuse from exterior surface to internal photocatalytic surface. Then their adsorption onto the surface takes place. The generation of reactant species is induced by UV-light illumination and consequent production of electrons and positive holes on the catalyst surface. Reactive species come into contact with the pollutants and break them down. Intermediates, which are produced during the photochemical reactions, can be eventually converted into CO_2 and water. Finally, products desorb from the surface, diffuse from

the interior catalyst pores to the external surface and after that to the main flow (Zhong & Haghighat 2015; Mamaghani et al. 2017).

Over the past decades, gas-phase photocatalysis has been studied and used for a wide array of chemicals removal. TiO_2 broad activity can be explained by the photogeneration of the strong oxidant, the hydroxyl radical, and reactive species (Mo et al. 2009).

For instance, photocatalytic oxidation helps to eliminate VOCs from the contaminated air under UV-light. Photocatalytic oxidation on catalyst surface is capable of breaking down various VOCs, such as alkanes, halo-alkanes, alkenes, halo-alkenes, aldehydes, alcohols, ketones and aromatics (Verbruggen 2015).

Namely, formaldehyde, acetaldehyde, acetone, benzene, m-Xylene, p-Xylene, o-Xylene, ethyl benzene, toluene, styrene, trichloroethylene and tetrachloroethylene can be removed from the gas stream. Depending on the light wavelength, the inlet concentration of VOCs and other factors, conversions can typically vary from 50% to 100% (Stevens et al. 1998; Pichat et al. 2000; Jo et al. 2002; Ao & Lee 2003; Jo & Park 2004; An et al. 2012).

Other studies were carried out to investigate the removal of other pollutant classes, such as gaseous SO_x, NO_x, CO, O_3, S-containing compounds, H_2S and dioxins (Zhao et al. 2009; Nishimura et al. 2010; Hassan et al. 2013; Lu et al. 2014; Yao & Feilberg 2015).

1.5.1 Air purification systems

Kinetic experiments have shown that the reaction rate of photocatalytic oxidation depends on light intensity, types and concentrations of pollutants, humidity levels, flow rate, catalyst and the reactor. Numerous scientific studies have predominantly concentrated on the structure and all of the other aspects which concern photocatalysts itself. However, knowledge of photocatalysts is not enough. In order to optimize and enhance the removal of pollutants, the knowledge of optimal operating conditions, constructions of photocatalytic reactors and air purifying appliances is also important, or even crucial. The most important parameters of reactors used for photocatalytic oxidation, e.g. VOC convective mass transfer rate, reaction surface area, should be studied and understood (Mo et al. 2009).

Typically, such reactor consists of a reaction surface and an UV source. It is advised that it should have a large reaction area and a low air velocity for a high mass transfer. The light should directly illuminate a photocatalytic surface. Medium pressure mercury lamps, xenon lamps, and UV-A lights (and even UV-LED) are the employed light sources. Various aspects should be taken into

consideration when designing an air purification system, among these: photocatalyst form (film, powder, foam, filter), quantum efficiency, UV source (its wavelength and power), light source distance from a catalyst surface, contaminant types and concentrations, gas flow type and rate (Ren et al. 2017).

Different types of reactors used for photocatalytic oxidation are known. These include powder layer, plate, honeycomb, annular, packed-bed, fluidized-bed, optical fiber, mop fan and combined-adsorption type reactors (Mo et al. 2009). The plate, honeycomb monolith and annular reactors are the most illustrative types.

In the *plate* type reactor, UV lamp is located parallel to photocatalyst layer, which is coated onto a plate surface. The construction is simple and the pressure drop is low. Large convective mass transfer rates and the reaction rates could be achieved, but the reaction area is quite small.

In the *honeycomb* type reactor, perforated substrate is coated with a photocatalyst, and the UV light is parallel to the reaction area. This leads to low reaction rates even if the reaction area and the mass transfer are sufficient. These have been used for the automobile exhaust emission control and for the reduction of NO_x in power-plant gases. They have a low pressure drop and a high surface-area-to-volume ratio.

The *annular* type reactor consists of two concentric cylinders that form an annual region with a gap. Photocatalyst is coated on the interior wall of cylinder. The geometry is quite simple, and the pressure drop is low. The convective mass transfer rate and the reaction area of the annular type reactor are small even if the direct illumination is present. The entrainment of catalyst can occur.

In *fluidized-bed* reactors, a gas flows through a catalyst bed. An illumination source can be internal or external to a reactor containing a photocatalyst bed. The advantages are the low pressure drop, the high gas feed rate, the high convective mass transfer rate and the efficient UV illumination.

Photocatalytic oxidation reactors could be utilized in HVAC (heating, ventilation and air conditioning) systems because they operate at ambient conditions and their compact design. Reactors have to be constructed in such way that no intermediates could cause a secondary pollution and harm the environment or humans. Energy consumption of different reactors should be also taken into consideration (Zhao & Yang 2003; Mo et al. 2009; Huang et al. 2016; Ren et al. 2017).

1.6 Photocatalytic coatings

Examples of widely studied and used catalysts primarily include metal oxides or sulphides, such as Al_2O_3, CdS, CeO_2, Fe_2O_3, porous Ga_2O_3, $In(OH)_3$, SnO_2, TiO_2, WO_3, ZnO, ZnS and ZrO_2. The most popular photocatalysts are TiO_2 (titania) and ZnO.

However, titania is the only suitable semiconductor which can be used for the industrial use due to its low price. No additional chemicals are required. TiO_2 has several crystal forms: anatase, rutile, brookite. Anatase is the most superior for the photocatalytic oxidation application. Very stable peroxide groups can be formed at anatase, but not at rutile. The energy band-gap (E_g) of anatase and rutile is 3.23 and 3.02 eV, respectively. Studies have shown that the anatase crystal form has better performance due to its more favorable conduction band configuration and stable surface peroxide groups. The commercial P25 (Evonik) consists of two crystals: anatase (70%) and rutile (30%) (Hashimoto et al. 2005; Mo et al. 2009).

TiO_2 photocatalysts can be of zero-dimensionality (spheres), one-dimensionality (fibers, tubes), two-dimensionality (nanosheets) and three-dimensionality (interconnected structure). Two-dimensional TiO_2 nanosheets have highly smooth flat surface, good hardness, excellent adhesion to substrates, antifouling properties, low turbidity, and they are applied in the field of self-cleaning coatings. Three-dimensional TiO_2 structures with pores have large surface-to-volume ratios (Nakata & Fujishima 2012).

1.6.1 Applications

TiO_2 photocatalysis is widely used not only for air and water purification, but it is also used in different other fields and products. These include self-cleaning surfaces, sterilization, hydrogen evolution, photoelectrochemical conversion and even cancer therapy (Fujishima et al. 2000; Nakata & Fujishima 2012).

Photocatalytic coatings can be regarded as self-cleaning and anti-fogging surfaces. The self-cleaning ability is the result of the combination of two photo-induced properties: the superhydrophilicity (high wettability) and the photocatalytic activity. These coatings have the ability to regenerate themselves in the contaminant-free air and under irradiation. Different surfaces can have more photocatalytic character and less superhydrophilic character, or vice versa - that depends on the composition and the processing of the surface. The longer the catalyst is irradiated with an UV light, the more organic material can be photodegraded. As a consequence, a stain on the surface, for example, can gradually disappear. It was also shown that if a TiO_2 film

is prepared with a certain percentage of SiO_2, it acquires high wettability after UV illumination. In this case, electrons and holes react differently. Electrons tend to reduce the Ti(IV) cations to the Ti(III) state, and the holes oxidize the O^{2-} anions. As a result, oxygen atoms are ejected, thus creating oxygen vacancies. Then, H_2O molecules attach to these oxygen vacancies, OH groups are produced and the surface becomes hydrophilic. After some time, water acquires the tendency to spread across the surface and drain from it (Fujishima et al. 2000).

Numerous scientific groups and companies, especially in Japan, have tried to utilize these properties for the benefit of the environment and human well-being. Some applications include self-cleaning tiles, paints, mirrors, windows and auto glass, construction materials (asphalt, pavement, wall), rear view mirrors, clothes, paper and steel (Ollis 2000; Banerjee et al. 2015). Pollutants which are present in the urban air could be removed via photocatalyst in building materials. These new generation building materials self-regenerate in the presence of rainwater, and the light source is the sunlight. Indoors, however, additional light source is required. Studies are being conducted in order to test the photocatalytic activity of these titania surfaces. It is important to test these materials (e.g. silicate, cement, glass, mortar, stone) directly on-site and under ambient and real-life conditions, since air pollution has various types of contaminants (Zhong & Haghighat 2014).

For example, the ability to purify the air from NO_x gases by self-cleaning concrete pavement with titania layer was investigated. The highest removal rate was observed at 25% relative humidity (Dylla et al. 2011). In another study in the Netherlands, the outdoor monitoring was done to compare the street with concrete pavement containing TiO_2 to the control street. It was found that the NO_x levels were lower, on average, by 19% (considering the whole day) and by 28% (considering only afternoons) compared to the control street values. In Rome, Italy, scientists have studied NO_x concentrations after the renovation work of the ‘‘Umberto I’’ tunnel. The tunnel vault was treated with a photocatalytically active cement-based paint. The results showed that a reduction of NOx values over 20% was achieved, particularly in the center of the tunnel, after two months of the tunnel renovation (Guerrini 2012).

The photocatalytic reactions can also be used as a method of disinfection and sterilization. For instance, the Ag-Ce-TiO_2 composite film has much higher antibacterial efficiency against *Escherichia coli* than glass and pure TiO_2 film either in the room light or in the dark (Zhang et al. 2009). In another study, Vohra et al. (2006) showed that Ag ion doped titania had the enhanced microbial destruction performance compared to a conventional TiO_2 photocatalyst. Photocatalytic oxidation (1) inhibits the proliferation of microorganisms, (2) provides disinfection,

(3) degrades the toxins produced and/or (4) eliminates the intermediates of contaminants. To apply this property of photocatalysis, photocatalytic tiles to cover the floor and walls could be used in operating rooms or in public bathrooms (Fujishima et al. 2000; Ren et al. 2017).

1.6.2 Templates addition and their influence on photoactivity

Photocatalytic activity and other properties of a photocatalyst could be improved, for example, by doping metal ions into TiO_2. Investigations clearly identify that doping transition metals, e.g. Co, Cr, Cu, Fe, Mn, Ni, V, into TiO_2 extends the response into the visible region. However, the photocatalytic performance in the UV region decreases. Doping of nonmetals, such as N or C, into TiO_2 also made it possible for visible light to activate the catalyst. Doping can narrow the band gap, create surface defects and change the grain size (Zang et al. 2000; Zhong & Haghighat 2015; Ren et al. 2017).

Accumulating evidence suggests that the doping of nanocrystalline TiO_2 with lanthanide ions (Eu^{3+}, La^{3+}, Nd^{3+}, Pr^{3+}, Sm^{3+}) significantly improves the photocatalytic performance. Lanthanide doping could narrow the band gap of TiO_2, so the absorption edges shift to the visible-light region and retain strong redox potentials (Wang et al. 2000; Bettinelli et al. 2006; Zhao & Liu 2008).

Non-porous TiO_2 has a low pollutant adsorption ability. In addition to this, water vapor can be competing with toxic chemicals for adsorption sites on a photocatalyst during photocatalytic oxidation. This drawback can be mitigated by inventing hybrid photocatalysts - composites of TiO_2 with adsorbents. Immobilizing titania on activated carbon (AC) helps reach a satisfactory pollutant removal rate even at high water vapor conditions. The effect of TiO_2/AC is more significant with decreasing residence time and increasing levels of humidity. Another benefit of using adsorbents is that produced intermediates are not released into the air since they are adsorbed and then further oxidized (Yoneyama & Torimoto 2000; Ao & Lee 2004).

In addition, TiO_2 photocatalysts can be coupled with metal oxides (e.g. Bi_2WO_6/TiO_2, ZnO/TiO_2, Al_2O_3/TiO_2, Ca_2SiO_4/TiO_2, $SiMgO_x/TiO_2$, BaO/TiO_2). These are more photocatalytically active compared to the non-modified titania. The migration of e^- and/or h^+ between transition Me oxide and TiO_2 prevents the recombination step.

A binary template of polyethylene glycol (PEG) and chitosan were used for the sol–gel synthesis of mesoporous titania. The samples preserved the anatase type titania. Moreover, they exhibited the highest photocatalytic activity for the photodegradation of 4-chlorophenol, in comparison with all the synthesized photocatalytic systems and P25. The presence of PEG and chitosan in the binary

template influenced the crystallite size, pore size and surface area of the photocatalyst and its catalytic activity. It was shown that PEG was responsible for mesopore formation (Preethi et al. 2014). Porous films can be more effective in removal of layers of some types of chemicals, which indicates that these films possess a self-cleaning property. The mesoporosity ensures fast transport of O_2 and H_2O onto the large catalyst surface (Zita et al. 2010).

Another study demonstrated that H_2SO_4 treatment of TiO_2 surface causes higher photocatalytic decomposition efficiency of gaseous toluene. H_2SO_4-treatment of TiO_2 also helped to mitigate catalyst deactivation. The reason for this could be the accelerated decomposition of intermediates by surface strong acid itself or resultant high quantum yield by decreasing the recombination between e^- and h^+ (Nakajima et al. 2005)**.**

The addition of SiO_2 can improve the photocatalytic activity and hydrophilicity of thin sol–gel layers of TiO_2, which influences both the crystallinity and the surface acidity. The higher the concentration of SiO_2, the smaller particle size of TiO_2 is. The type of additive can play an important role in determining the properties of thin films. TiO_2/SiO_2 self-cleaning films could be used on glass and ceramic materials. They can be easily converted by weak UV-illumination into superhydrophilic state. They are resistant to abrasion and have good photocatalytic activity. TiO_2 films modified with polydimethylsiloxane (PDMS) are more hydrophobic than the TiO_2/SiO_2 ones. They exhibit developed micro-mesoporosity, and different photocatalytic activity (low or high), depending on the chemical being tested (Novotná et al. 2007).

Moreover, SiO_2 can act as a barrier between a substrate (glass) and a TiO_2 film. Alkali ions, especially Na^+, are not tightly bound in a glass substrate. They can diffuse from glass during the calcination process and negatively affect the photocatalytic activity of the film. If sodium concentration is low, it could act as a recombination center, lowering the e^- and h^+ density and inhibiting the radicals formation. If levels are high, other crystalline phase, like brookite or sodium titanate, can emerge, which is not desirable, since the photocatalytic property of titania depend on the high amount of crystalline anatase. In order to avoid Na^+ diffusion, (1) a barrier can be introduced, (2) the glass nature could be changed (borosilicate instead of soda lime glass) or (3) the treatment temperature could be decreased during the anatase phase synthesis (Krýsa et al. 2011; Aubry et al. 2012). However, borosilicate glass is more expensive than soda-lime glass, which should be taken into account. In Zita, Maixner and Krýsa (2010) study, it was shown that TiO_2 layers with SiO_2 barrier have photocatalytic activity more than 20 times higher than those without a barrier. Another study showed that using SiN_x as a barrier can be even more efficient than SiO_2 (Aubry et al. 2007).

1.6.3 Deactivation

It is observed that gas–solid photocatalyst activity typically decreases with time, and catalyst deactivation occurs. There are several reasons for this phenomenon: (1) less active photocatalyst sites due to adsorption of intermediates, (2) blockage of pores by fouling, (3) photopolymerization of some chemicals on the surface, especially in the absence of water, and (4) complete photooxidation of species with N and S heteroatoms with subsequent accumulation of oxidized inorganic forms of N and S. However, often it is quite hard to pinpoint the true reason for catalyst deactivation (Ollis 2000; Mo et al. 2009).

Luckily, some regeneration techniques have been investigated and reported. These include (1) exposing photocatalyst to pure or humid air, (2) irradiating the photocatalyst with UV irradiation, (3) applying a vaporized H_2O_2 solution to the catalyst, (4) exposing the catalyst to different temperatures, (5) using chloride radical system and (6) ozone-purging in the presence of humidity. However, in some cases, some photocatalysts cannot be regenerated (Mo et al. 2009).

1.6.4 Methods of preparation

The methods for TiO_2 preparation could be grouped into two sections: gas-phase methods and liquid-phase methods.

The first liquid-phase method is *sol-gel*. In this colloidal chemistry method, porous TiO_2 anatase coatings are prepared from alkoxide solutions which contain organic polymer. Alkoxide solutions and organic polymer are mixed in the sol solution. The method consists of titanium alkoxides $Ti(OR)_4$ hydrolysis and polycondensation. A liquid (the sol) is chemically transformed into a gel state. After that, transition into solid oxide material happens. The chemical control of these reactions allows the formation of monodispersed powders, thin films or fibers directly from the solution at lower temperatures. The advantages of this method are low processing temperature and molecular-level homogeneity. The use of PEG as a polymeric fugitive compound in the production of TiO_2 films is an efficient method of producing porous thin films. Decomposition of PEG in the gel at 520 °C leads to the generation of pores in these coatings. The porosity of films improves their photocatalytic activity (Yu et al. 2000; Mo et al. 2009; Ramírez-Santos et al. 2012).

The next technique is the *liquid-phase hydrolysis of* $TiCl_4$. The technique has been used commercially in order to manufacture TiO_2 in fine particulate form. $TiCl_4$ is soluble in cold water, and the hydrolysis reaction takes place rapidly at mild temperatures.

The overall reaction chemistry is (Reactions 11, 12):

$TiCl_4 + 2H_2O \rightarrow TiO_2$ (anatase) + 4HCl (11)

$TiCl_4 + 2H_2O \rightarrow TiO_2$ (rutile) + 4HCl (12)

These reactions can occur in parallel, but the second reaction is more thermodynamically favorable (Mo et al. 2009).

TiO_2 can also be prepared using the *hydrothermal method*. In this method of TiO_2 powder preparation, liquid solutions as solvents are used to produce the precursors under high temperature (usually <250 °C) and high-pressure. The hydrothermal conditions have crucial effects on the formation, phase component, morphology, and particle size of produced titania. After being washed and dried, TiO_2 powders are obtained. $TiCl_4$ or ($Ti(SO_4)_2$) can be used as a precursor. A solution of NaOH or ethanol and water are the typical solvents. As a result of the process, uniform nanometer rutile and anatase particles can be obtained (Cheng et al. 1995; Mo et al. 2009).

The technique, known as *water-in-oil microemulsion*, can be also employed for the preparation of photocatalysts. Microemulsions are transparent, optically isotropic and thermodynamically stable colloidal dispersions. Water and oil coexist in one phase due to the presence of surfactant molecules with balanced hydrophilic-lipophilic properties. An aqueous droplet serves as a nanoreactor and the synthesized particles cannot grow bigger than the micelle. The drawback of this method is that the oil phase can pollute the surface of the particle. Post-treatment is usually applied (Mo et al. 2009).

One of the gas-phase methods of titania preparation is the *gas-phase oxidation of $TiCl_4$*. Titania powders may be also produced via oxidation of volatile metal chlorides at high temperature and near atmospheric pressure conditions using industrial flame-aerosol reactors. In flame synthesis, the formation of TiO_2 particles starts from the homogeneous nucleation of a stable cluster of gaseous molecules of titania. After that, the cluster begins to grow because of the condensation of molecules onto its surface. The reaction chemistry is as follows (Reactions 13, 14):

$TiCl_{4(g)} + O_{2(g)} \rightarrow TiO_{2(g)} + 2Cl_2$ (13)

$nTiO_{2(g)} \rightarrow (TiO_2)_{n(s)}$ (14)

The particle morphology and size are influenced by the chemical reaction pathways (gas phase and/or surface), nucleation type (homogeneous and heterogeneous), transport effects (which can lead to particle agglomeration or deposition onto surfaces) and sintering (Zeatoun & Feke 2005).

The other known technique is the *gas-phase hydrolysis of titanium alkoxides*. The vapors of titanium alkoxides ($Ti(OR)_4$) and H_2O are sprayed with nitrogen gas into a hydrolysis chamber. Spherical TiO_2 particles are formed as a result of the hydrolysis. Hydrolysis may be represented by these steps (Mo et al. 2009):

$$Ti(OR)_{4(g)} + 4H_2O_{(g)} \rightarrow Ti(OH)_{4(s)} + 4ROH_{(g)} \quad (15)$$

$$Ti(OH)_{4(s)} \rightarrow TiO_2 \cdot H_2O_{(s)} + H_2O_{(g)} \quad (16)$$

$$TiO_2 \cdot H_2O_{(s)} \rightarrow TiO_{2(s)} + H_2O_{(g)} \quad (17)$$

The advantages of gas-phase methods include control of stoichiometry, grain-size, morphology and orientation; physicochemical homogeneity, atomic-level mixing and interaction. The drawbacks are the need for expensive equipment, vacuum conditions. The advantages of liquid-phase methods, in addition to those stated above for the gas-phase, are greater flexibility in form (e.g. films, powders, foam) and inexpensive processes (Ren et al. 2017).

After the photocatalyst preparation, it is typically coated onto the surface. There are several types of TiO_2 coating methods. One of the most popular methods is *dip-coating* (or wash-coating). In this method, the flat substrate (ceramic, glass or silica plate) is immersed into a sol and then withdraw with a certain speed. A sol film is then formed on the substrate. The thickness of a film is influenced by the withdrawal speed, the solid content and the viscosity of the liquid. Temperature and other factors are controlled during the process. The adhered sol is left to dry in open atmosphere at the room temperature. This stage is called gelation (densification), and the solvent is evaporated. The film is then further dried in an oven. Methods of angle-dependent dip coating, spin coating or flow coating are also used in practice. Coating methods also have an effect on the photocatalytic activity (Sonawane et al. 2004; Mo et al. 2009).

2 Experimental part

2.1 Materials and methods

2.1.1 Experimental set-up

The experiments in present study were conducted in a multi-section continuous-flow type reactor (Fig. 3). The reactor consisted of five sections, which were placed parallel to each other and affixed to the wall. Sections were connected to each other with tubes to allow for the inlet and outlet flow. The tubes were equipped with valves to open or close the air flow. Above every section, one irradiation source (lamp) was positioned. Each section of the reactor had the volume of 130 milliliters, giving 650 milliliters for the whole reactor. Each reactor had a plate, on which the photocatalyst soda-lime plates were laid out. The surface area of photocatalytic coatings in each reactor was 120 cm^2, giving the surface area of 600 cm^2 in total for all five reactors.

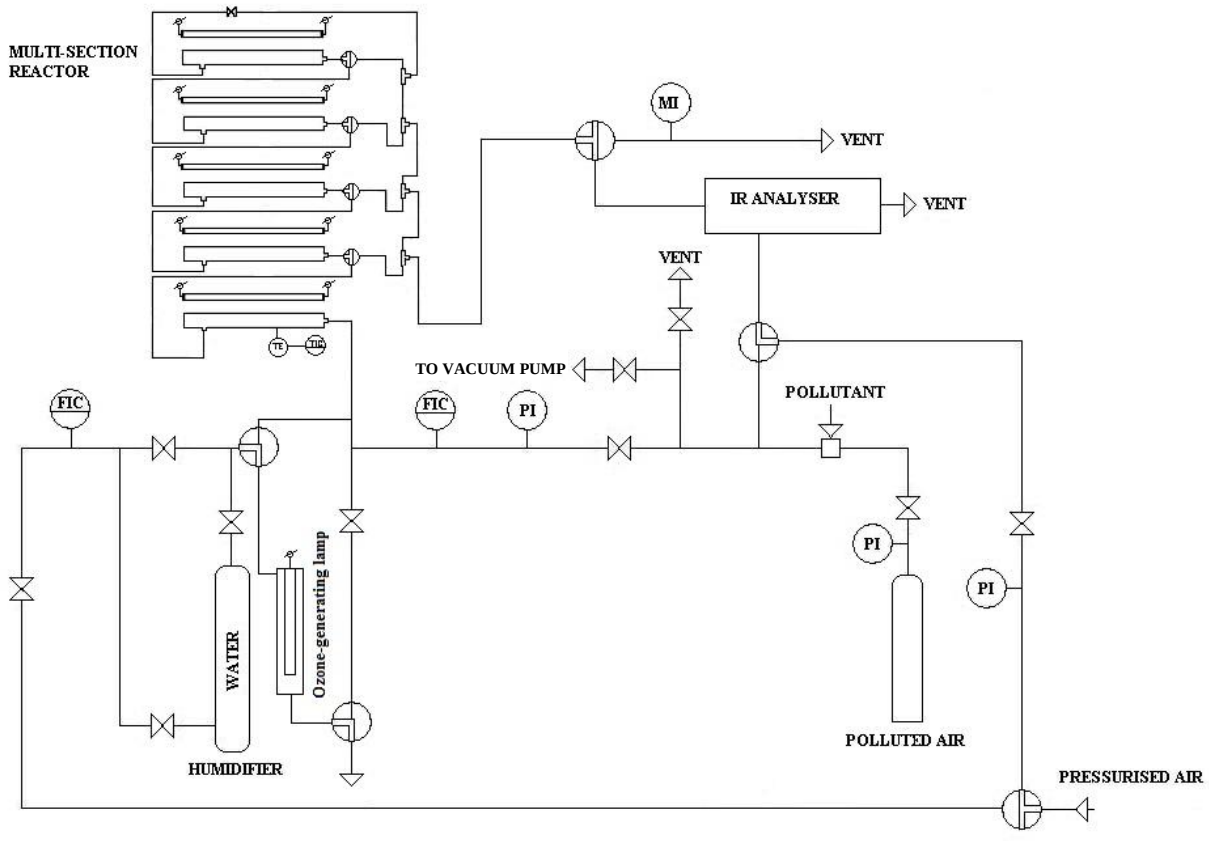

Figure 3. The scheme of the experimental set-up used for the gas-phase photocatalytic degradation of MTBE

(TE – thermocouple, TIC - temperature indicator controller, FIC - flow indicating controller, MI - humidity indicator, PI – pressure indicator)

Cylinder gas tank was employed for polluted air storage. Air humidifier was used in one series of the experiment to increase air humidity in the gas flow. Another crucial part of the set-up was INTERSPEC 200-X Fourier-transform infrared spectrometer (FTIR), which helped to determine contaminant species and their content in the outlet flow. In addition, two flow indicating controllers for diluent and polluted air, vacuum pump, thermocouple, humidity and pressure indicators were utilized to tune the set-up and conduct the experiment correctly.

2.1.2 Materials and analyses

Thin titania films used in the study were synthesized by Tallinn University of Technology PhD student Natalja Pronina in Clausthal University of Technology (TU Clausthal). First of all, the barrier SiO_2 layers, which were intended to be coated onto soda-lime glass, were synthesized. These were prepared via sol-gel method from 5.2 g of tetraethyl orthosilicate (TEOS), 10 g of 2-propanol, 1 g of water and 1 g 1 M HNO_3, diluted by 2-propanol to 3.5% of SiO_2. After the preparation, TEOS-based thin films were deposited onto glass by dip-coating (1 mm s^{-1}) method and dried at 200 °C for 10 min. Coating thickness of barrier layer was measured to be ca. 54 nm. Finally, the anatase titania thin films were obtained by sol-gel method from TBOT, stabilized by ethylacetoacetate (mol 1:1) and diluted with 2-propanol to get a titanium dioxide concentration of 4.7%. These were coated onto soda-lime glass with barrier films by dip-coating (1 mm s^{-1}) and consolidated for 30 min at 500 °C. Coating thickness of TBOT-based thin films was measured to be ca. 64 nm. They were templated with stearic acid, which concentration in sol was 3%. Resulted coating thickness of templated TiO_2 films was measured to be ca. 80 nm.

The titania coatings were characterized by X-ray diffraction (XRD, Siemens D5000 Kristalloflex), secondary neutral mass spectrometry (SNMS, INA-X from Specs GmbH Berlin), UV-VIS absorption (Perkin Elmer Lambda 950 UV/Vis/NIR spectrometer) and Scanning Electron Microscopy (SEM, Zeiss EVO 50 and Field emission SEM Dual-Beam Helios Nanolab 600, FEI) at TU Clausthal.

In present study, MTBE was the pollutant which was used for studying photocatalytic activity of TiO_2 thin films. The efficiency of MTBE degradation was investigated based on its concentration in outlet flow. MTBE peaks were measured at the infrared (IR) bands from 1063 to 1124 cm^{-1} by the aid of FDM VPFTIR HiRes quantitative spectra library. In addition, the concentration of the produced intermediate, tert-butyl formate (TBF), was also analyzed. TBF peaks were measured at the IR bands from 1138 to 1190 cm^{-1}. The air spectra were taken using software Interspec 3.40 Pro and processed by Essential FTIR software.

MTBE degradation was also examined under no-light conditions as a reference. As expected, zero contaminant conversion was observed under these conditions.

The conversion of MTBE was calculated from the following equation (Equation 1):

$$Conversion\ (\%) = \frac{C_{in} - C_{out}}{C_{in}} \times 100\% \quad \text{where,} \qquad (1)$$

C_{in} – MTBE concentration at reactor inlet, ppm

C_{out} – MTBE concentration at reactor outlet, ppm

2.1.3 Photocatalytic experiments

The aim of the experimental runs was to investigate how different process-influencing factors affect the photocatalytic removal of pollutant, MTBE. Photocatalytic oxidation series were carried out at the temperature of 34 °C in a multi-section continuous-flow type reactor (Fig. 3).

First, the mixture of air with the contaminant was prepared in 50 L gas tank. In order to do this, suitable volume (V) of MTBE was calculated by injection calculator (Equation 2) and injected through the injection port under vacuum conditions.

$$V[\mu L] = \frac{\frac{P+14.7}{14.7} \times V_{tank}}{R \times T} \times M \times C_m \times \frac{0.000001}{\rho \times 0.001} \quad \text{where,} \qquad (2)$$

P – filling pressure, 44 psig

V_{tank} – VOC feed tank volume, 50 L

R – gas constant, 0.08206 L atm mol^{-1} K^{-1}

T – temperature, 293.15 K

M – molecular weight, 88.15 g mol^{-1} for MTBE

C_m – desired concentration, ppm

ρ – density, 0.75 g mL^{-1} for MTBE

One of the varied factors was MTBE inlet concentration. The desired concentration of the pollutant in some series of the experiments was 10 ppm, in others 25 ppm (Table 3).

The injected pollutant was left under vacuum at least for 20 minutes for evaporation. Next, compressed air was let into the tank until pressure of 3 bars was reached. Concentration balancing in the tank proceeded for 1.5 hours.

After that, in one series of the experiments, polluted air was let pass through the humidifier. Relative humidity in the air was registered by a humidity meter (TPI597 Digital Hygrometer), and

reached 35±5%. In other series, the relative humidity of air, which was not additionally humidified, was registered to be 5±1%.

Air from compressed air line (ambient air) was taken as a reference by FTIR spectrometer in all series. Then, polluted air was let out of tank, and its MTBE concentration was analyzed in the by-pass line. Finally, polluted air was introduced into the reactor for photocatalytic oxidation. The concentration of MTBE was measured in outlet air flow after passing one, two, three, four and five sections of the photocatalytic system. All IR spectra were taken after 10 and 20 minutes of experimental run.

In some series, air flow was varied from 0.5 to 1 L min^{-1}, which corresponds to the residence time of 15.6 and 7.8 s per one reactor section, respectively. Gas flow was monitored by a flow indicating controller (Omega FMA 5400/5500). Instead of the residence time per section, another term could be more suitable – specific residence time, which is measured in s cm^{-2}. It is typically used for the evaluation of reactor photocatalytic performance. It can be calculated by dividing residence time by the surface area of photocatalytic coating. If air flow is increased, then residence time in section decreases, thus specific residence time is also diminished. Specific residence time in this study was varied from 0.065 to 0.13 s cm^{-2}.

Another varied influencing condition was irradiation source – either UV-A light or visible light. Artificial UV-A irradiation was provided by UV Philips Actinic BL 15 W lamps, irradiance 3.5 mW cm^{-2} with reflector (integrated in the range of 180 - 400 nm, with max emission at 365 nm, UV-B/UV-A ratio < 0.2%). As a visible light source, VIS Philips TL-D 15 W lamps were used, irradiance 3.3 mW cm^{-2} with reflector (integrated in the range of 180 - 700 nm, UV/UV-VIS ratio < 5%). The photocatalytic coating was lit all the time during the experiment.

Table 3. Experimental series carried out in present study for the gas-phase photocatalytic degradation of MTBE

Series number	**Flow rate, L min^{-1}**	**Specific residence time, s cm^{-2}**	**MTBE concentration, ppm**	**Relative humidity, %**	**Irradiation source**
1	0.5	0.13	10	5±1	UV-A
2	0.5	0.13	25	5±1	UV-A
3	0.5	0.13	10	35±5	UV-A
4	0.5	0.13	10	5±1	VIS
5	1	0.065	10	5±1	UV-A
6	1	0.065	25	5±1	UV-A

3 Results and discussion

The photocatalytic activity of templated TiO_2 thin photocatalytic film (TBOT-5-SA-3) which was coated onto barrier layer of SiO_2 was studied. The substrate for the barrier and photocatalytic layers was common soda-lime glass. About 90% of today's glass is soda-lime glass, typically used for windows, light-bulbs, bottles, glasses, plates. It is composed of 60-75% SiO_2, 12-18% sodium oxide (soda) and 5-12% calcium oxide (lime). Its resistance to corrosive chemicals is average and resistance to high temperatures is rather poor (The Corning Museum of Glass 2011). The purpose of SiO_2 barrier layers is to protect titania, since, unfortunately, soda-lime glass tends to potentially poison (deactivate) the photocatalyst with Na^+ ions (Krýsa et al. 2011). It was also decided to study TiO_2 templated with stearic acid, which amount was 3% in sol. Stearic acid is a basic template which is widely used to improve photocatalytic activity of titania films (Xu et al. 2002; Chen et al. 2008).

The results of present study were intended to show the dependence of TiO_2 thin film photocatalytic oxidation activity on different influencing factors, such as irradiation source, pollutant specific residence time and concentration, relative humidity levels. Higher photocatalytic activity of the film is indicated by higher MTBE conversion. Any presence of intermediates in the outlet signals incomplete oxidation. Higher (or complete) pollutant conversions and the lack of intermediates are the desirable outcomes of any oxidative removal process.

The results of this study will be compared to the ones obtained with TBOT-4 photocatalytic coatings prepared on borosilicate glass plates and investigated in the Master thesis of Jekaterina Spiridonova (Spiridonova 2016). All the experimental series in both studies were carried out at same operating conditions to allow the results to be compared (Table 3). For the purpose of comparison, soda-lime plates in present study were coated with SiO_2 barrier layer, and the layer of titania was templated with stearic acid, unlike borosilicate plates with untemplated titania layers used in the work of Jekaterina Spiridonova. Borosilicate glass, also known as pyrex, is usually 80% SiO_2, 13% B_2O_3, 4% total alkali, 2% Al_2O_3. It is heat-resistant because of its low thermal expansion coefficient. It has high resistance to chemical corrosion. Good qualities of this type of glass is attributed to boron oxide and various other specialty elements. However, it is not as low in cost as soda-lime glass. Borosilicate glass has a vast array of uses ranging from cookware to laboratory ware, implantable medical devices, pipelines and devices used in space exploration (Sell 1992; The Corning Museum of Glass 2011).

Although soda-lime glass poisons the photocatalyst, and the application of barrier layer complicates the coating of glass with titania (even though SiO_2 synthesis is not time-consuming or technologically complicated process), the difference in price of soda-lime and borosilicate glass justifies the scientific interest towards the coatings with barrier layers on soda-lime. The price of an ordinary soda-lime glass sheet with a 2-mm thickness is 13.61 EUR m^{-2} (Klaas24.ee 2017), as opposed to borofloat glass price of \$11.25 ft^{-2} or about 110.62 EUR m^{-2} for 2 mm plate (S.I. Howard Glass Co. 2013).

3.1 Characterization of photocatalytic titania coating TBOT-5-SA-3 in comparison with TBOT-4

TBOT-5-SA-3 and TBOT-4 photocatalytic coatings were thoroughly studied. X-ray diffraction (XRD), secondary neutral mass spectrometry (SNMS), UV-VIS absorption and Scanning Electron Microscopy (SEM) analyses were carried out at Clausthal University of Technology.

3.1.1 XRD

Characterization of the crystallite phase of titania coatings can be done with XRD analysis. XRD method is one of the most powerful scientific techniques for identifying and quantifying crystalline materials. Anatase and rutile are the stable phases of TiO_2. Since 1950s, quantitative analysis of a mixture of these phases has been possible by means of XRD (Sakurai & Mizusawa 2010).

Figure 4 shows the XRD patterns of TBOT-5-SA-3/SiO_2 catalysts as well as of TBOT-4. The reflections at 2θ values of 25.3°, 36.9°, 37.9°, 38.2°, 48.1°, 54°, 55.2°, 62.8°, 69.9°, 70.2°, 75.3°, and 83.2° are attributed to anatase-phase TiO_2, whereas reflections at 2θ values of 27.4°, 36.1°, and 41.2° indicate rutile-phase TiO_2 (ICSD 2017). As observed from XRD patterns, TBOT-5-SA-3/SiO_2 catalyst has four anatase peaks, no rutile peaks could be observed.

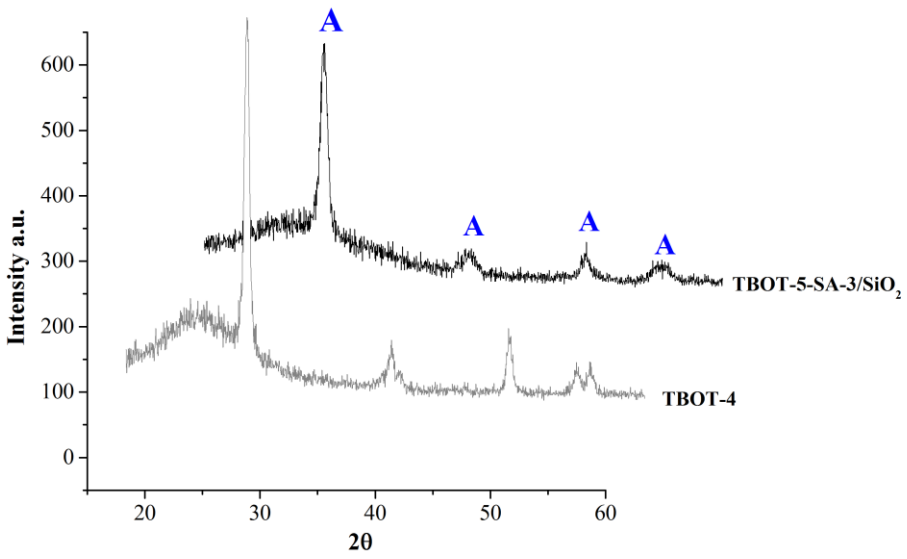

Figure 4. X-ray diffraction pattern of titania coatings (A – anatase peak)

3.1.2 SNMS

SNMS analysis enables to determine the depth composition and distribution of a photocatalytic coating. During the analysis, the surface of a sample is bombarded by an ion beam. Because of this bombardment, neutral atoms are released. These are detected by a mass spectrometer after some post-ionization. As a result of the analysis, a depth profile can be generated, which shows intensities of various present elements, starting from surface and advancing inwards (Vad et al. 2009; Lee 2012). Figure 5 shows the obtained data from SNMS analysis. It is evident from the figure that during the first 200 seconds Ti can be seen both in TBOT-4 and TBOT-5-SA-3/SiO_2. In case of TBOT-4, oxygen is the second seen atom, and Na content rises sharply after 200 s. As for the templated coating, it has a bigger amount of Na towards its surface than TBOT-4, which was expected due to Na diffusion from soda-lime glass. However, the Ti intensity in the templated coating is still higher than Na intensity.

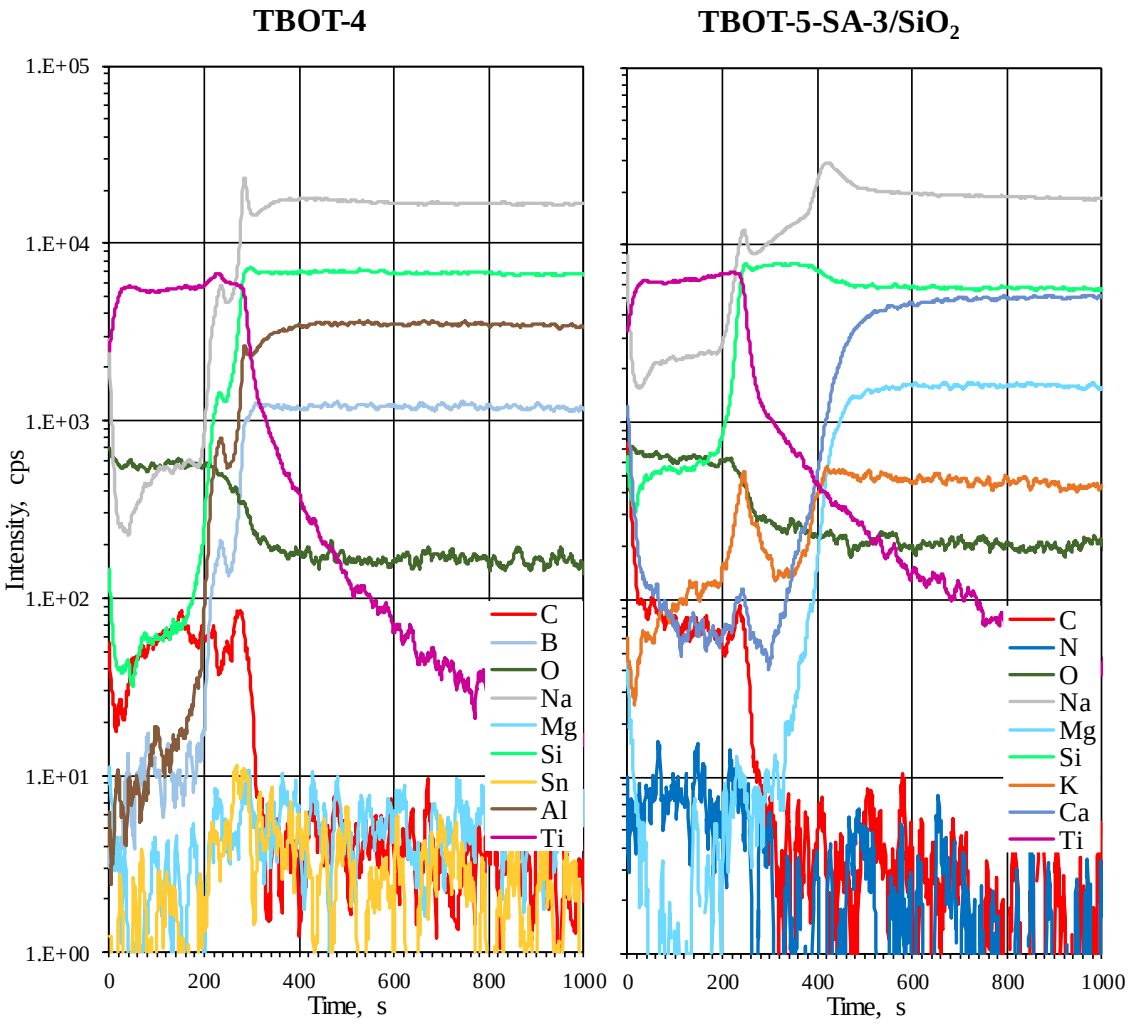

Figure 5. SNMS surface analysis data

3.1.3 UV-VIS absorption

UV-VIS absorption spectroscopy measures the attenuation of a light beam after it has passed through a specimen or has reflected from the specimen's surface. It can be carried out at one single wavelength or over an extended region of the light. When the light gets absorbed, it excites the electrons to higher energy state orbitals. The more easily they are transitioned, the less energy it is required for their excitation (PharmaXChange.info 2011). UV-VIS transmission of titania coatings is depicted in figure 6. It can be seen from the results that pyrex and float glass transmit more UV light than the plates with the coatings. It can be seen from the figure that the transmission percent of TBOT-5-SA-3/SiO2 on float glass is less than that one of float glass, and has a shift in the UV-A region of the plot. Nonetheless, the templated film still is capable of light transmission, and does it even better than TBOT-4.

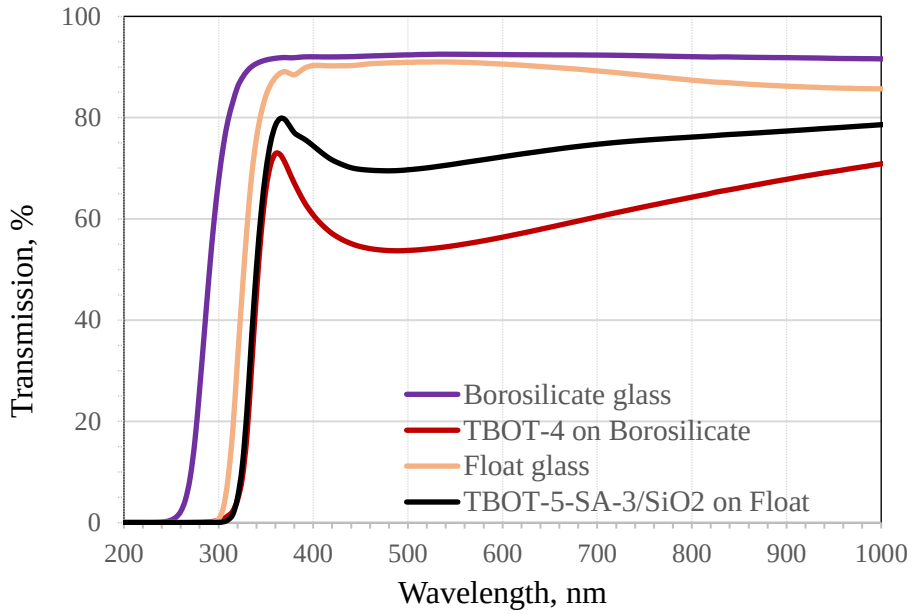

Figure 6. UV-VIS transmission of titania coatings

3.1.4 SEM

The surface morphology of titania coatings was evaluated by employing SEM (Fig. 7). This method may also give information about chemical composition, crystalline structure and orientation of materials. It uses a beam of high-energy electrons to obtain images of a sample by producing a variety of signals at the surface of the sample. A selected area or a point on the surface can be studied. As a result, 2-dimensional image is produced that shows spatial variations in the properties (National Science Foundation 2017).

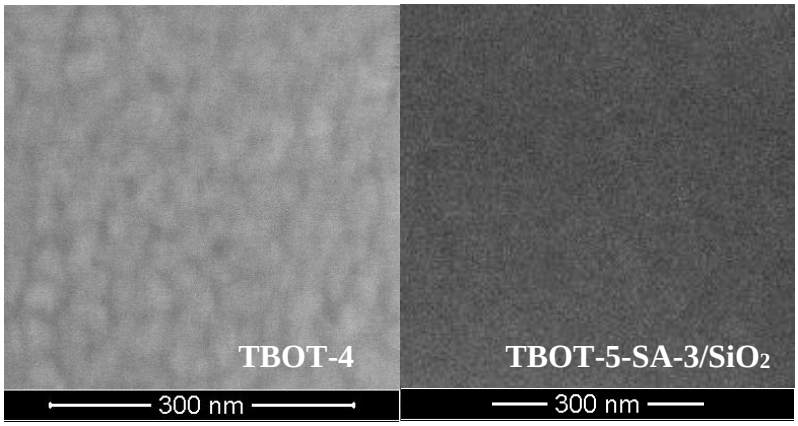

Figure 7. FESEM and SEM images of titania coatings

Figure 7 displays the SEM images of titania coatings, and it can be seen that the coatings are fairly uniform, without any cracks, and the surface is smooth. The images were taken using different instruments - FE SEM and SEM techniques. The first one enables to see individual crystallites. The quality of the second one does not allow that, although the uniformity can still be seen.

3.2 Influence of MTBE concentration

One of the many factors which influence the performance of the photocatalytic process is the contaminant type and its concentration on the reaction surface. Different pollutant concentrations lead to different reaction rates. For every experimental series, the optimal pollutant concentration exists. The pollutant most effective conversion will be achieved if the optimal concentration is found and if other factors are taken into account. Inlet concentration may be different from the one that is on the reaction surface of a photocatalyst because of the insufficient convective mass transfer. Usually, it is observed that higher concentrations of VOCs lead to improved reaction kinetics, lower removal efficiencies and incomplete mineralization (Mo et al. 2009; Mamaghani et al. 2017).

Present study compares the series in which MTBE concentration is different while the other factors are not changed. The specific residence time of both series is 0.13 s cm^{-2}, relative humidity is 4-6% and UV-A lamps are at work. The inlet concentration of the first series is 10 ppm and the concentration of the second is 25 ppm (Fig. 8).

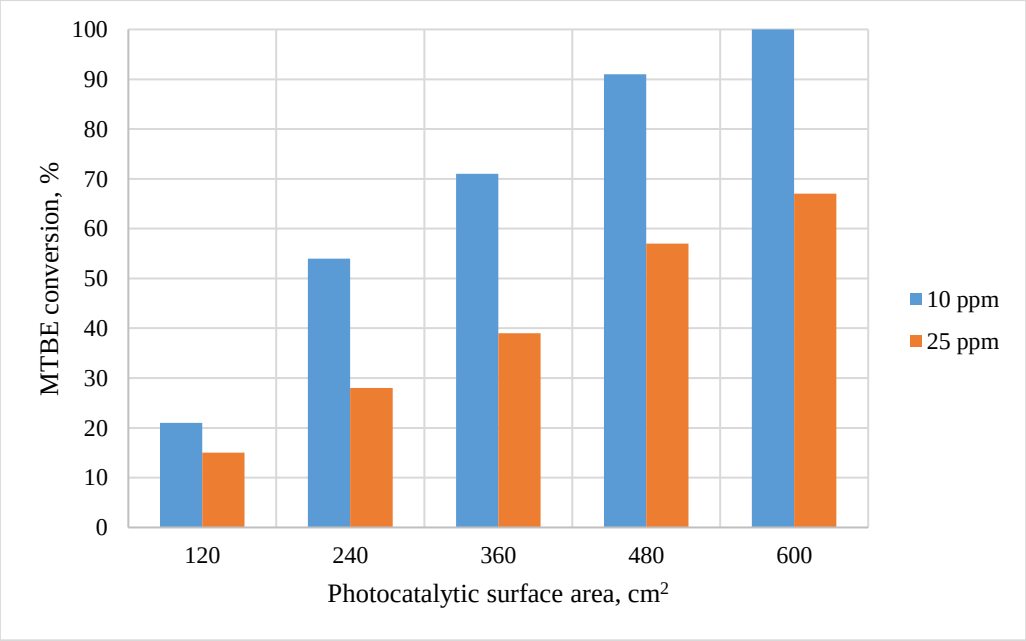

Figure 8. Influence of MTBE inlet concentration on photocatalytic performance of TBOT-5-SA-3

Figure 8 reveals that using higher inlet MTBE concentration results in smaller conversions (orange columns). In case of 10 ppm concentration, it was possible to achieve 100% pollutant conversion with titania surface area of 600 cm^2. Using 480 cm^2 area gave the conversion of 91%. In case of 25 ppm, the maximum achieved conversion after 5 sections of the reactor was 67%.

In Jekaterina Spiridonova experiments, TBOT-4 coating completely oxidized the pollutant in both series. The area of 480 cm^2 was enough for 100% conversion with 10 ppm concentration, while the area of 600 cm^2 was needed to reach the same result for 25 ppm.

The content of the intermediate (TBF) was higher for 25 ppm: rising and reaching the maximum value of 3.4 ppm after four sections, and then falling to 2.5 ppm after five sections (Fig. 9). Thus, further increase in the surface area of photocatalytic coatings will lead to the mineralization of higher amount of pollutant. In case of 10 ppm, the highest value of TBF was 0.9 ppm, which steadily declined to almost zero level if let through 5 sections of the reactor system.

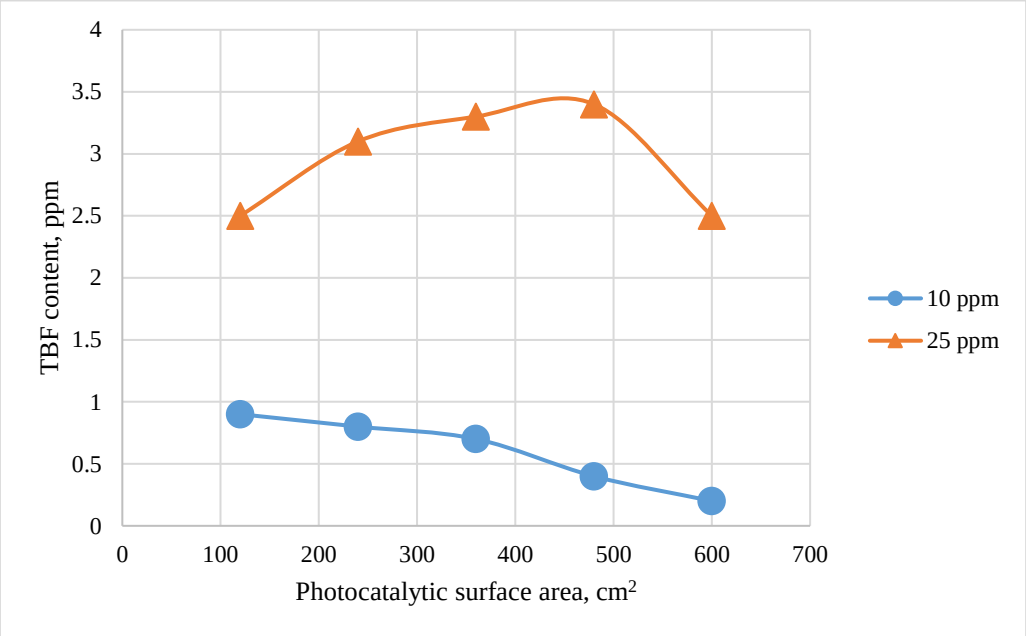

Figure 9. Influence of MTBE inlet concentration on the content of intermediate oxidation product TBF

As far as TBOT-4 is concerned, the intermediate was completely degraded at 62.4 s of residence time (corresponding to 480 cm^2) for 10 ppm, and at 78 s (corresponding to 600 cm^2) for MTBE inlet concentration of 25 ppm, although much higher gas-phase concentrations of TBF (up to 5 ppm) were observed at lower residence times.

It can be concluded that smaller MTBE concentrations are preferable in order to completely oxidize the pollutant and its intermediate oxidation by-products. TBOT-5-SA-3 was able to completely degrade 10 ppm of MTBE with 600 cm^2 catalyst area. The system with TBOT-4 coatings was able to perform complete photocatalytic oxidation in both series, for 10 ppm as well as 25 ppm.

3.3 Influence of air humidity

Another crucial factor in photocatalysis process is the air humidity. Water molecules produce hydroxyl radicals when they react with the positive holes on the activated photocatalyst surface. These radicals react with pollutant molecules and convert them into the intermediates and finally into H_2O and CO_2. If water vapor is absent, total mineralization of compounds into CO_2 may not occur. If the air humidity is too high, then the water molecules can compete with other compounds. They may prevent other molecules from contacting the photocatalyst surface by blocking the surface-active sites or competing with contaminants for adsorption. Thus, photocatalytic reaction rate is reduced. This competitive adsorption was observed for various pollutants, such as toluene, formaldehyde and acetone. In addition to this, at very high levels of the air humidity, vapor can block UV and lower its intensity. Consequently, relative humidity can either positively or negatively affect the photodegradation rate. Usually, there is an optimal air humidity level that could maximize photocatalytic oxidation reaction rate. Some studies found that as VOC concentration increases, higher levels of humidity may be beneficial. Mineralization, intermediates type and amount can be also affected by varying relative humidity levels (Huang et al. 2016; Mo et al. 2009; Zhao & Yang 2003; Mamaghani et al. 2017).

Current study used two experimental series with different air humidity levels in order to consider its influence on the degradation process of MTBE (Fig. 10). Specific residence time (0.13 s cm^{-2}), MTBE concentration (10 ppm) and irradiation source (UV-A) were the same in both series.

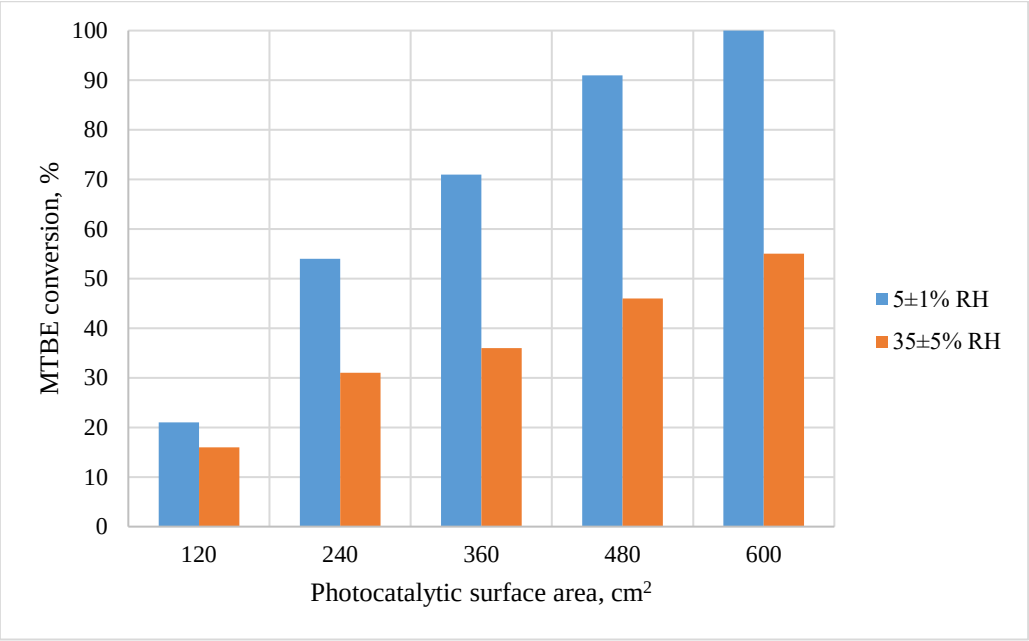

Figure 10. Influence of air humidity on photocatalytic performance of TBOT-5-SA-3 (RH – relative humidity)

In present study, it was found that higher relative humidity levels of 35±5% had a quite negative impact on the oxidation process, compared to 5±1% levels (Fig. 10). The higher catalyst area only slightly increased the MTBE removal if RH was high: 600 cm^2 allowed for 55% conversion. In contrast, when air humidity level was 5±1%, it was possible to achieve total degradation of MTBE within the whole reactor system.

Study with TBOT-4 coatings revealed only slight variations in pollutant degradation with the increase of RH from 6 to 35%. For instance, for catalyst surface area of 360 cm^2, MTBE conversions only differed from each other by 5% at different RH levels, reaching 75% and 80% at RH of 6% and 35%, respectively.

In oxidation process with TBOT-5-SA-3, higher humidity levels caused higher TBF outlet concentrations, as can be seen in figure 11. As an exception, for catalyst area of 120 cm^2, TBF amount was about the same for both runs. For the area of 600 cm^2, the difference was distinguishable: ca. 0.2 ppm for 5±1% RH, and 1.8 ppm for 35±5% RH.

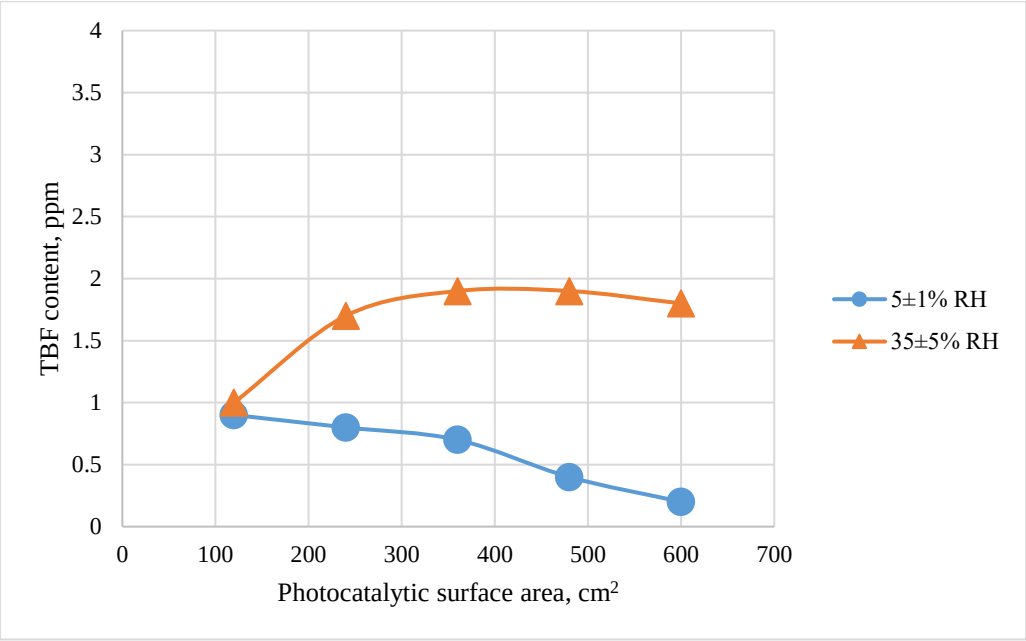

Figure 11. Influence of air humidity on TBF content (RH – relative humidity)

In oxidation process with TBOT-4, it was noticed that the content of TBF was always higher at higher humidity levels. The final content for five sections, however, was lower than 0.5 ppm for 6% RH, and ca. 3 ppm for 35% RH.

It was clear from the results, that high RH leads to significant decline in MTBE conversions for TBOT-5-SA-3, but not so notably for TBOT-4. For both coatings, it is evident that elevated RH has a detrimental effect on the mineralization of TBF.

3.4 Influence of irradiation source

Irradiation source and intensity are one of the key influence factors in photocatalytic oxidation, since it provides the energy which is needed to overcome the band gap (3.2 eV in titania) in a photocatalyst. In theory, titania photocatalyst is activated by the UV light with the wavelength less than 380 nm. Other types of photocatalysts which can be activated by the visible light region are also being developed and studied. The most popular lamps utilized for photocatalytic oxidation are germicidal lamps (UVC, 254 nm) and fluorescent black-light lamps (300-400 nm). Although higher light intensity usually favors the pollutant removal, excessive light intensity reduces quantum efficiency and not economically justified (Mo et al. 2009; Mamaghani et al. 2017).

In present research, in order to study the importance of irradiation in MTBE oxidation process, the series with UV-A lamps were compared to the visible light series (Fig. 12). Other factors, such as

specific residence time (0.13 s cm^{-2}), inlet concentration (10 ppm) and relative humidity (4-6%) were kept constant.

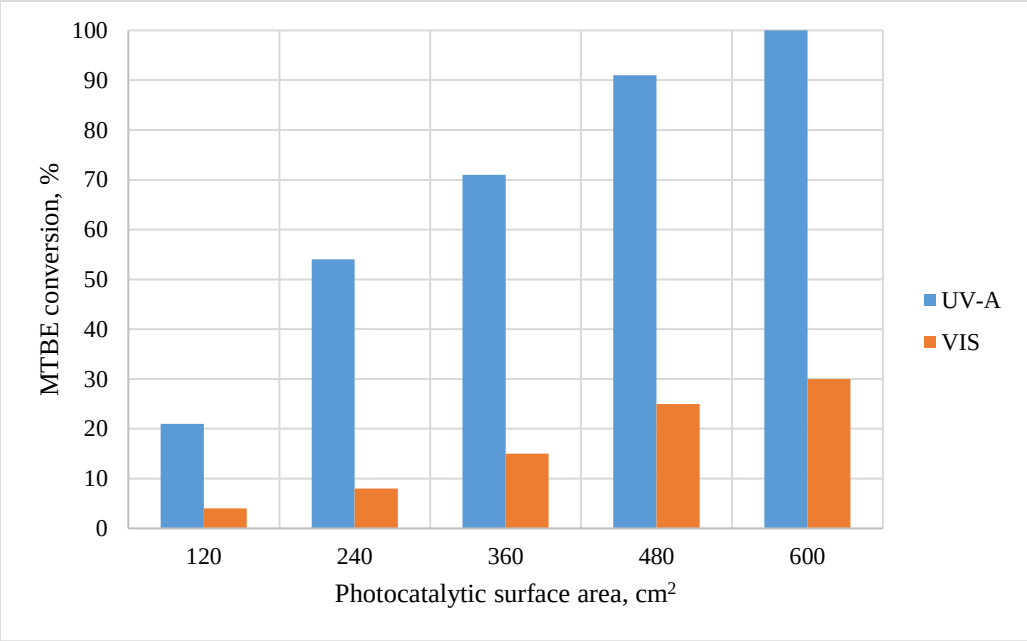

Figure 12. Influence of irradiation source on photocatalytic performance of TBOT-5-SA-3

Figure 12 illustrates the influence of irradiation source on MTBE degradation. It is apparent from the chart that the choice of light source plays a noticeable and significant role in the process. Unsurprisingly, MTBE conversions under UV-A irradiation conditions were always much higher than the conversions under VIS light. Five sections together were capable of degrading all MTBE content under UV-A light. Nonetheless, degradation still took place under VIS light, starting at 4% for the catalyst area of 120 cm^2, and achieving 30% for the area of 600 cm^2.

TBOT-4 films showed the same trends. At residence time of 78 s (catalyst surface area of 600 cm^2), MTBE conversion was 47% under VIS light, while UV-A irradiation led to the entire degradation.

Results for TBF content after MTBE oxidation with TBOT-5-SA-3 film may be inspected in figure 13. Under UV-A light (blue line), the highest TBF amount was in the beginning of the experimental run, reaching ca. 1 ppm for the catalyst area of 120 cm^2. After that, it started to gradually decrease with the incorporation of other reactor sections, hitting its low of 0.2 ppm. Under VIS light (orange line), TBF concentration started out at 0.6 ppm, increased up to 1.5 ppm and remained almost unchanged (1.4 ppm at 600 cm^2).

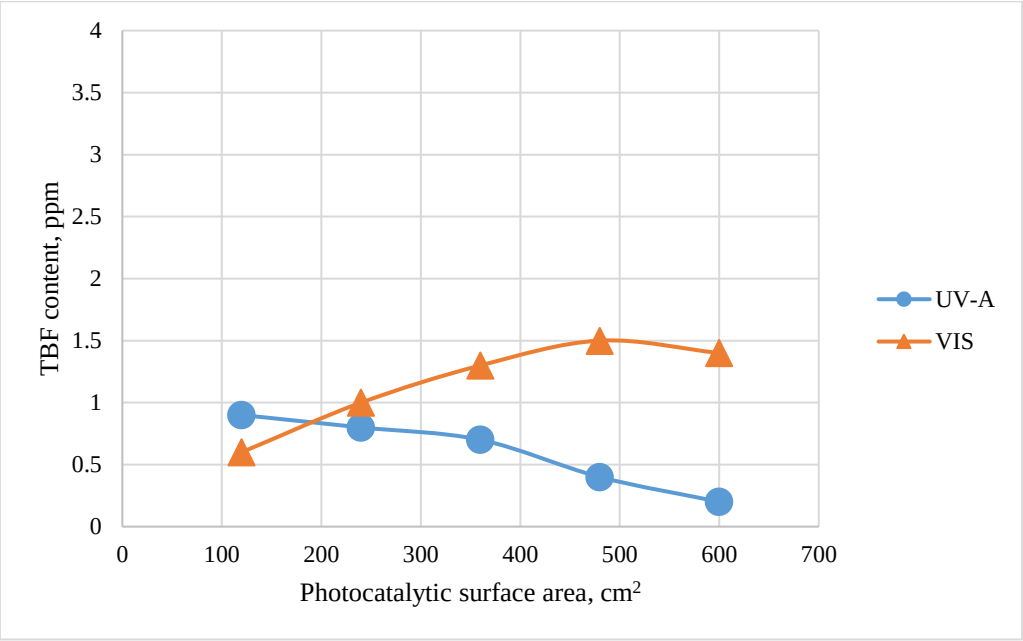

Figure 13. Influence of irradiation source on TBF content

TBOT-4 coatings also allowed for the accumulation of TBF under VIS light conditions, leveling off at 6 ppm. UV-A was more effective for MTBE photocatalytic degradation than VIS light: the peak was at 4.7 ppm and then dramatically plummeted to final 0 ppm.

Thus, UV-A light was more effective in MTBE removal than VIS light in all experiments. TBOT-4 films were 17% more effective than TBOT-5-SA-3 ones at surface area of 600 cm^2 under VIS light conditions. Interestingly, final TBF concentration was, on the other hand, higher for TBOT-4 - 6 ppm, unlike 1.4 ppm for TBOT-5-SA-3.

3.5 Influence of specific residence time

In addition to the factors listed above, the flow rate and therefore the specific residence time, also affect the performance of photocatalytic process. When the photocatalytic oxidation is controlled by the gas-phase mass transfer, the reaction rate increases with the increase in the flow rate. If it is controlled by the surface reaction, the higher flow rate leads to lower conversion rate. Usually, higher air flow rates reduce the contact time between contaminants and reactive species, and negatively influences the removal efficiency (Zhao & Yang 2003; Zhong & Haghighat 2015).

In current study, different series of experiment with different flow rates, and thus, specific residence time values were conducted. The compared flow rates were 0.5 and 1 L min^{-1}.

The residence time was 0.13 and 0.065 s cm^{-2}, respectively. MTBE concentration, relative humidity of 4-6% and UV-A light irradiation were maintained the same.

Altogether, four series were carried out: two with different specific residence time values and inlet MTBE concentration of 10 ppm; and other two with different specific residence time values, but with 25 ppm inlet MTBE concentration. As a result, it was possible to evaluate the influence of specific residence time on the pollutant mineralization in case of two various pollutant concentrations.

Figure 14 shows the obtained data for two distinct specific residence time values in case of 10 ppm MTBE concentration and TBOT-5-SA-3 thin film. It can be seen from the figure that longer specific residence time yields higher MTBE conversions. The photocatalyst surface area of 600 cm^2 allowed for 100% MTBE conversion at specific residence time of 0.13 s cm^{-2}. Reduction in specific residence time to 0.065 s cm^{-2} resulted in significant decrease in MTBE conversion. The same catalyst area now allowed for total 67% conversion (the last orange column).

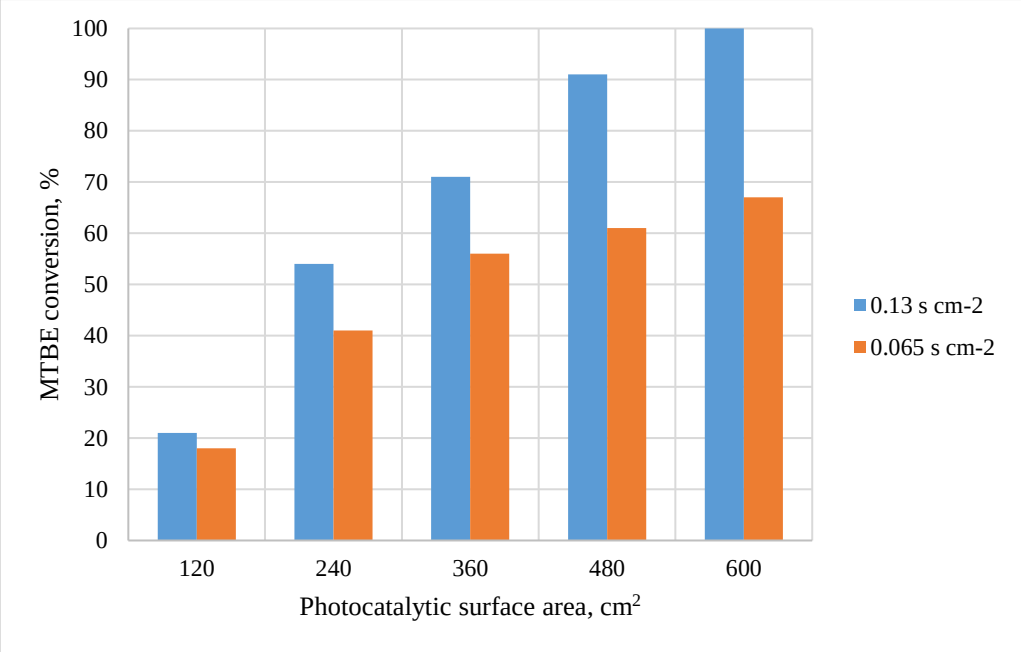

Figure 14. Influence of specific residence time on photocatalytic performance of TBOT-5-SA-3; MTBE inlet concentration 10 ppm

The total residence time of 15.6 s can be achieved after first section in case of specific residence time of 0.13 s cm^{-2}. The same residence time is achieved after two sections in case of specific residence time of 0.065 s cm^{-2}. Given that the residence time is 15.6 s, using shorter specific

residence time, and thus larger photocatalyst area, is more advantageous than using longer specific residence time but smaller surface area (41 vs 21% conversion).

The total residence time of 31.2 s can be achieved after two sections in case of specific residence time of 0.13 s cm^{-2}. The same residence time is achieved after four sections in case of specific residence time of 0.065 s cm^{-2}. The difference between MTBE conversions with different specific residence time values but with the same total residence time of 31.2 s in this case is smaller (about 5%) but still present. Consequently, increasing airflow and dividing the process between sections, where flow rates are changing entering and exiting the tubing, enhances the mass transfer of MTBE. The bigger surface area has more available active sites, which in turn can oxidize more molecules.

It was found that TBF concentration was about the same for two different specific residence time values (Fig. 15). For both series, the fluctuations in TBF content were less than 1 ppm. Starting at 240 cm^2 photocatalytic area, the intermediate concentration was a little bit higher for the specific residence time of 0.065 s cm^{-2}, and since MTBE conversions were smaller this indicates lower mineralization of pollutant at shorter specific residence time if same photocatalytic surface areas are in use.

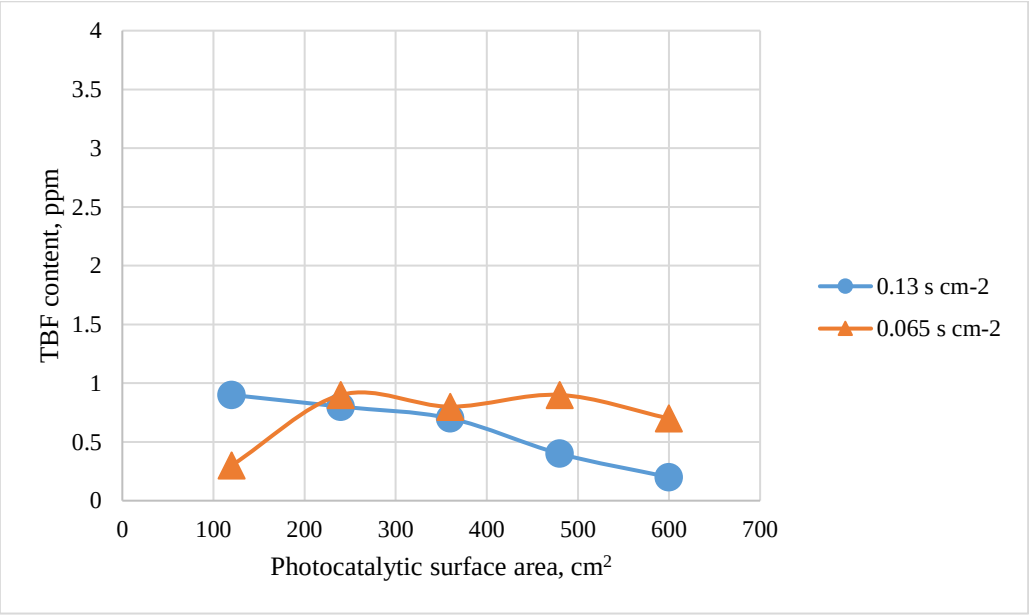

Figure 15. Influence of specific residence time on TBF content; MTBE inlet concentration 10 ppm

The next two figures (Fig. 16 and 17) will describe the trends in MTBE conversion and TBF concentration for the series with TBOT-5-SA-3 films, where pollutant concentration was chosen to be 25 ppm and was kept constant. Specific residence time values were only varied.

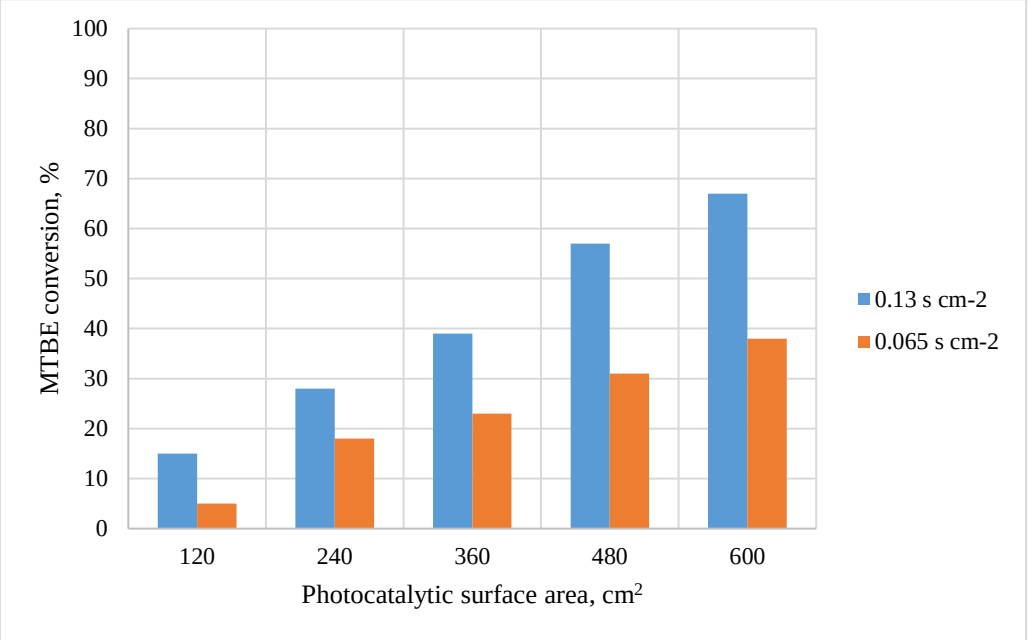

Figure 16. Influence of specific residence time on photocatalytic performance of TBOT-5-SA-3; MTBE inlet concentration 25 ppm

As was expected, series with longer specific residence time (0.13 s cm^{-2}) had higher conversions (Fig. 16) if same areas of photocatalytic coatings are compared. The progressive conversion increase can be observed, and the catalyst surface area of 600 cm^2 allowed for the 67% of MTBE conversion. The gradual increase in contaminant conversion is also true for the specific residence time value of 0.065 s cm^{-2}. However, the surface area of 600 cm^2 allowed for much smaller MTBE conversion of 38%.

If the residence time is 15.6 s for both experimental runs, then the MTBE conversion for the specific residence time of 0.13 s cm^{-2} is 15%, and for the specific residence time of 0.065 s cm^{-2} – 18%, i.e. are similar at both regimes. If the residence time is higher (31.2 s), then the conversion for the specific residence time values of 0.13 and 0.065 s cm^{-2} are once again about the same – 28 and 31%, respectively. It seems that the higher inlet concentration of MTBE is, the less significant the effect of mass transfer becomes, and the process is limited by the surface reaction.

For the same MTBE concentration of 25 ppm, the process of mineralization on TBOT-4 films was much more effective. For example, with longer specific residence time (0.13 s cm^{-2}), final MTBE conversion reached 100% after all five sections of the reactor were used. When the specific residence time was decreased to 0.065 s cm^{-2}, the maximum conversion of 81% was reached.

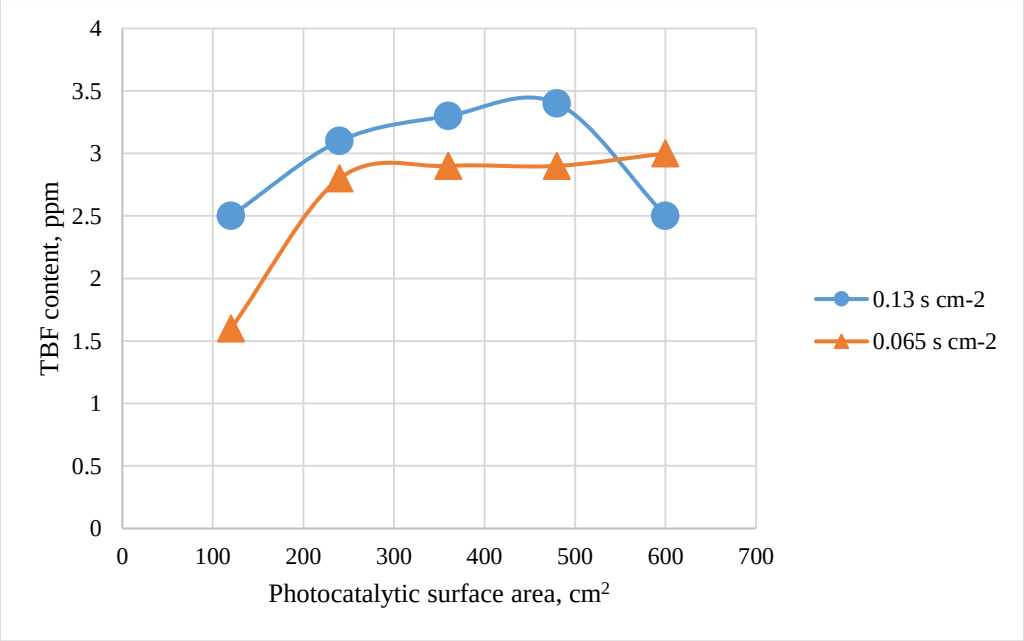

Figure 17. Influence of specific residence time on TBF content; MTBE inlet concentration 25 ppm

The use of longer specific residence time resulted in higher TBF content. It was increasing from the beginning until it started to decline from the peak of 3.4 ppm to 2.5 ppm after the incorporation of fifth section of the reactor. When the specific residence time was shorter, TBF content, at first, increased and then leveled out at about 2.9 ppm. It was not declining in the end because the MTBE conversion was still relatively small and growing, indicating incomplete mineralization of MTBE and TBF.

In case of TBOT-4 at the same conditions, specific residence time of 0.13 s cm^{-2} caused the total intermediate compound mineralization if all five sections were used. The peak of 4.7 ppm was reached in the second section of the reactor. Shorter specific residence time was the reason for higher TBF content, peaking at 7.8 ppm in the third section and declining to 3.7 ppm after the fifth section.

In conclusion, it can be stated that overall conversions of MTBE in series with TBOT-5-SA-3 films were higher if MTBE initial inlet concentration was smaller, which confirms the previous findings in chapter 'Influence of MTBE concentration'. As a result of this, TBF content was smaller because photocatalytic oxidation was more effective.

As far as the influence of template and substrate is concerned, TBOT-4 on borosilicate glass was more effective than TBOT-5-SA-3 under various specific residence time values. As an example, the coating on borosilicate glass could completely convert 25 ppm of MTBE into CO_2 and H_2O with longer specific residence time. In comparison, the templated coating converted 67% of MTBE. In addition to this, 2.5 ppm of the intermediate were still present in the outlet gas flow.

Although the results of SNMS analysis indicated that SiO_2 barrier layer can diminish the diffusion of Na ions to the surface, Na content may be still high enough to undermine the photocatalytic activity of a templated coating. It may be hypothesized that the use of double protection layer may further enhance the photocatalytic activity of a film. Future experimental research should be dedicated to the investigation of this assumption.

Conclusions

The goals of present Master thesis were to (1) present the literature review of air pollutants, methods of air purification, gas-phase photocatalysis and photocatalytic coatings, and to (2) experimentally investigate the photocatalytic performance of titania coatings in a multi-section continuous-flow type reactor, and analyze the influence of various factors on the process of pollutant degradation.

First, main air contaminants and their effects on human health were reviewed. Methyl tert-butyl ether (MTBE), the volatile organic compound (VOC), was reviewed in more detail. Air pollutants are the cause of millions of annual deaths worldwide. They are also responsible for the increased risk of various degenerative diseases and some types of cancer. Secondly, the particular emphasis was put on the explanation of gas-phase photocatalytic oxidation and its mechanism. Main advantages and disadvantages of this process were discussed. In addition to this, modifications of air treatment systems utilized specifically for this method were briefly described. Thirdly, photocatalytic coatings were thoroughly reviewed. Applications of self-cleaning coatings were outlined. The thesis provides some information on different templates added to photocatalytic coatings, and their influence on photocatalytic activity.

The second part of the thesis provided the description of the experimental set-up, materials used in the study and the experimental runs. The experiments were carried out to investigate the photocatalytic oxidation of MTBE in a five-section gas-phase reactor using TBOT-5-SA-3/SiO_2 photocatalyst. Each section had the volume of 130 mL and the titania surface area of 120 cm^2. During the study, the influence of various factors, such as MTBE concentration, air humidity, irradiation source and specific residence time, on photocatalytic activity of the coatings was explored.

The characterization of TBOT-based films and the results of the experiments were given in the third chapter. Based on the results, a number of conclusions about the performance of TBOT-5-SA-3 coatings under various conditions can be put forward:

- Using lower inlet MTBE concentration resulted in higher MTBE conversion and lower by-product (tert-butyl formate, TBF) content, which was the desirable outcome. For instance, it was possible to achieve 100% pollutant conversion with titania surface of 600 cm^2 and inlet MTBE concentration of 10 ppm. The surface of 480 cm^2 was enough to achieve the same result using TBOT-4 coatings.

- The increase in air humidity levels had a significant negative impact on the process of MTBE degradation. The whole reactor allowed for only 55% MTBE conversion with higher air humidity levels. However, the photocatalytic performance of TBOT-4 coatings were much less dependent on air humidity, and only slight variations in conversions were observed. Water molecules may have competed with the pollutant molecules for the adsorption and partially prevented them from contacting the catalyst surface area.
- Templated coating TBOT-5-SA-3 was found to be photocatalytically active under VIS light. However, it was possible to completely degrade MTBE under UV-A light conditions using the whole reactor, whereas VIS light allowed for 30% MTBE conversion. TBOT-4 coatings showed the same trends and performed even better under VIS light compared to templated coatings.
- As was expected, longer specific residence time values yielded significantly higher MTBE conversions. However, given the same residence time period, using shorter specific residence time results in higher conversions due to more efficient mass transfer, and more photocatalytic area is employed with its larger number of free photoactive sites. The same can be concluded about TBOT-4 films, however, their performance was overall better.

The use of SiO_2 barrier layer in TBOT-5-SA-3 coatings diminishes the diffusion of Na ions from soda-lime glass plate to the surface of the film. However, the results showed that more expensive borosilicate glass, which does not poison titania with Na ions, is the better substrate for the coatings. Higher conversions of MTBE can be reached using this type of glass. Unfortunately, it is much more expensive than the ordinary soda-lime. Therefore, the photocatalytic experiments on soda-lime glass are justified. Further research should be dedicated to the development of more photocatalytically effective coatings, for example by adding double barrier layers or special templates.

Resümee

Käesoleva magistritöö eesmärgid olid: (1) anda kirjanduse alusel ülevaade õhu saasteainetest, õhu puhastusmeetoditest, gaasifaasi fotokatalüüsist ja fotokatalüütilistest kiledest ning (2) eksperimentaalselt uurida TiO_2 kilede fotokatalüütilist toimimist viiesektsioonilises pideva vooluga reaktoris ja analüüsida erinevate tegurite mõju saasteaine lagundamisprotsessile.

Esiteks anti ülevaade põhilistest õhu saasteainetest ning nende mõjust inimtervisele. Teadaolevalt põhjustavad need ülemaailmselt mitu miljonit surmajuhtumit aastas. Saasteainetest käsitleti detailsemalt metüültert-butüüleetrit (MTBE). Teiseks vaadeldi lähemalt gaasifaasi fotokatalüütilist oksüdatsiooni, selle eeliseid, puuduseid ning mehhanisme. Kolmandaks kirjeldati üksikasjalikult fotokatalüütilisi kilesid ning nendega seotud aspekte, näiteks rakendusi. Magistritöö teine peatükk andis kirjelduse katseseadmest, kasutatud materjalidest ja eksperimentaalsetest seeriatest. Kolmandas peatükis toodi välja TBOT-baasil sünteesitud kilede iseloomustus ja katsete tulemused.

Tulemuste põhjal saab teha järgmisi järeldusi erinevate tegurite mõjust TBOT-5-SA-3 katete fotokatalüütilisele aktiivsusele:

- Madalam MTBE algkontsentratsioon põhjustas kõrgemat MTBE konversiooni ja madalamat vaheprodukti (tert-butüülformiaadi, TBF) teket. Näiteks saavutati lähteaine 100%-line konversioon, kui fotokatalüütiline pindala oli 600 cm^2 ja MTBE algkontsentratsioon - 10 ppm. Sama tulemus saavutati kasutades TBOT-4 katteid pindalaga 480 cm^2.
- Suhtelise õhuniiskuse suurendamine mõjutas MTBE lagundamisprotsessi negatiivselt. Reaktori kõikide sektsioonide kasutamisel oli võimalik saavutada ainult MTBE 55%-line konversioon, kui suhteline õhuniiskus oli suurem. TBOT-4 kilede fotokatalüütilise aktiivsuse sõltuvus õhuniiskusest oli aga väiksem. Vee molekulid võisid adsorptsiooni käigus konkureerida saasteaine molekulidega ning selle kaudu takistada nende kokkupuudet katalüsaatori pindalaga.
- Leiti, et TBOT-5-SA-3 kate on nähtava valguse käes fotokatalüütiliselt aktiivne. MTBE täielik lagundamine oli võimalik UV-A valguse käes kasutades kogu reaktorit, kusjuures nähtav valgus andis vaid MTBE 30%-lise konversiooni. TBOT-4 katted näitasid sama trendi ning nende aktiivsus oli võrreldes TBOT-5-SA-3 katetega nähtava valguse käes isegi kõrgem.

- Nagu oli arvata, põhjustas pikem eriviibimisaeg märgatavalt kõrgemat MTBE konversiooni. Seevastu, kui viibimisaeg oli muutumatu, põhjustas lühem eriviibimisaeg suuremat konversiooni just efektiivse massiülekande ja suurema pindala tõttu. Sama on järeldatav TBOT-4 katete kohta, kuid nende aktiivsus oli TBOT-5-SA-3 omast siiski kõrgem.

SiO_2 kiht TBOT-5-SA-3 katetes vähendas Na-ioonide difusiooni tavalisest klaasist (sooda-lubi-liivklaas) katalüsaatori pinnale. Tulemused näitasid aga, et borosilikaadist klaasplaat on parem substraat õhukeste kilede jaoks ning sellega on võimalik saavutada kõrgemaid MTBE konversioone. Katsed tavalise sooda-lubi-liivklaasiga on sellegipoolest põhjendatud ka tulevikus, kuna see on märkimisväärselt odavam klaasi liik.

Acknowledgements

I wish to express my sincere gratitude to my supervisor Marina Kritševskaja, Senior Research Scientist at the Department of Materials and Environmental Technology of TUT, for her great support, feedback, and help with preparation of present Master thesis.

Bibliography

An, T. et al., 2012. Synthesis of carbon nanotube–anatase TiO_2 sub-micrometer-sized sphere Composite Photocatalyst for Synergistic Degradation of Gaseous Styrene. *ACS Applied Materials & Interfaces*, 4(11), pp.5988–5996.

Ao, C.H. & Lee, S.C., 2003. Enhancement effect of TiO2 immobilized on activated carbon filter for the photodegradation of pollutants at typical indoor air level. *Applied Catalysis B: Environmental*, 44(3), pp.191–205.

Ao, C.H. & Lee, S.C., 2004. Combination effect of activated carbon with TiO_2 for the photodegradation of binary pollutants at typical indoor air level. *Journal of Photochemistry and Photobiology A: Chemistry*, 161(2–3), pp.131–140.

Aubry, E. et al., 2007. Poisoning prevention of TiO_2 photocatalyst coatings sputtered on soda-lime glass by intercalation of SiN_x diffusion barriers. *Surface and Coatings Technology*, 201(18), pp.7706–7712.

Aubry, E. et al., 2012. Effect of Na diffusion from glass substrate on the microstructural and photocatalytic properties of post-annealed TiO_2 films synthesised by reactive sputtering. *Surface & Coatings Technology*, 206, pp.4999–5005.

Banerjee, S., Dionysiou, D.D. & Pillai, S.C., 2015. Self-cleaning applications of TiO_2 by photo-induced hydrophilicity and photocatalysis. *Applied Catalysis B, Environmental*, 176-177, pp.396–428.

Bettinelli, M. et al., 2006. Photocatalytic, spectroscopic and transport properties of lanthanide-doped TiO_2 nanocrystals. *Journal of Physics: Condensed Matter*, 18(33), pp.S2149–S2160.

Block, M.L. et al., 2012. The outdoor air pollution and brain health workshop. *NeuroToxicology*, 33(5), pp.972–984.

Brinke, J. Ten et al., 1998. Development of new volatile organic compound (VOC) exposure metrics and their relationship to "sick building syndrome" symptoms. *Indoor Air*, 8(3), pp.140–152.

Brook, R.D. et al., 2002. Inhalation of fine particulate air pollution and ozone causes acute arterial vasoconstriction in healthy adults. *Circulation*, 105(13), pp.1534–1536.

Chen, C. et al., 2008. Photocatalytic degradation of C.I. Acid Orange 52 in the presence of Zn-doped TiO_2 prepared by a stearic acid gel method. *Dyes and Pigments*, 77(1), pp.204-209.

Cheng, H. et al., 1995. Hydrothermal preparation of uniform nanosize rutile and anatase particles. *Chemistry of Materials*, 7(4), pp.663–671.

Chin-Chan, M., Navarro-Yepes, J. & Quintanilla-Vega, B., 2015. Environmental pollutants as risk factors for neurodegenerative disorders: Alzheimer and Parkinson diseases. *Frontiers in Cellular Neuroscience*, 9, p.124.

Choi, J.S., Song, I.K. & Lee, W.Y., 2000. Performance of double-pipe membrane reactor comprising heteropolyacid catalyst and polymer membrane for the MTBE (methyl tert-butyl ether) decomposition. *Journal of Membrane Science*, 166(2), pp.159–175.

Curtis, L. et al., 2006. Adverse health effects of outdoor air pollutants. *Environment international*, 32(6), pp.815–830.

Dales, R.E. et al., 2004. Influence of outdoor aeroallergens on hospitalization for asthma in Canada. *Journal of Allergy and Clinical Immunology*, 113(2), pp.303–306.

Demeestere, K. et al., 2008. Heterogeneous photocatalytic removal of toluene from air on building materials enriched with TiO_2. *Building and Environment*, 43(4), pp.406–414.

Dylla, H. et al., 2011. Laboratory investigation of the effect of mixed nitrogen dioxide and nitrogen oxide gases on titanium dioxide photocatalytic efficiency in ooncrete pavements. *Journal of Materials in Civil Engineering*, 23(7), pp.1087–1093.

Environmental Pollution Centers, 2017. Radioactive Pollution Causes. Available at: https://www.environmentalpollutioncenters.org/radiation/causes/ [Accessed March 28, 2017].

François, A. et al., 2002. Biodegradation of methyl tert-butyl ether and other fuel oxygenates by a new strain, Mycobacterium austroafricanum IFP 2012. *Applied and environmental microbiology*, 68(6), pp.2754–62.

Fujishima, A., Rao, T.N. & Tryk, D.A., 2000. Titanium dioxide photocatalysis. *Journal of Photochemistry and Photobiology C: Photochemistry Reviews*, 1(1), pp.1–21.

Gordian, M.E. et al., 1995. Health effects of methyl tertiary butyl ether (MTBE) in gasoline in Alaska. *Alaska medicine*, 37(3), pp.101–3, 119.

Graue, B. et al., 2013. The effect of air pollution on stone decay: the decay of the Drachenfels trachyte in industrial, urban, and rural environments—a case study of the Cologne, Altenberg and Xanten cathedrals. *Environmental Earth Sciences*, 69(4), pp.1095–1124.

Greaver, T.L. et al., 2012. Ecological effects of nitrogen and sulfur air pollution in the US: what do we know? *Frontiers in Ecology and the Environment*, 10(7), pp.365–372.

Guerrini, G.L., 2012. Photocatalytic performances in a city tunnel in Rome: NO_x monitoring results. *Construction and Building Materials*, 27(1), pp.165–175.

Hashimoto, K., Irie, H. & Fujishima, A., 2005. TiO_2 photocatalysis: A historical overview and future prospects. *Japanese Journal of Applied Physics*, 44(12), pp.8269–8285.

Hassan, M. et al., 2013. Sustainable photocatalytic asphalt pavements for mitigation of nitrogen oxide and sulfur dioxide vehicle emissions. *Journal of Materials in Civil Engineering*, 25(3), pp.365–371.

Huang, R.-J. et al., 2014. High secondary aerosol contribution to particulate pollution during haze events in China. *Nature*, 514(7521), pp.218–222.

Huang, Y. et al., 2016. Removal of indoor volatile organic compounds via photocatalytic oxidation: a short review and prospect. *Molecules*, 21(1), p.56.

ICSD, 2017. ICSD Web. Available at: https://icsd.fiz-karlsruhe.de [Accessed May 8, 2017].

Jo, W.-K., Park, J.-H. & Chun, H.-D., 2002. Photocatalytic destruction of VOCs for in-vehicle air cleaning. *Journal of Photochemistry and Photobiology A: Chemistry*, 148(1), pp.109–119.

Jo, W.-K. & Park, K.-H., 2004. Heterogeneous photocatalysis of aromatic and chlorinated volatile organic compounds (VOCs) for non-occupational indoor air application. *Chemosphere*, 57(7), pp.555–565.

Jones, A.P., 1999. Indoor air quality and health. *Atmospheric Environment*, 33, pp.4535–4564.

Joseph, P.M. & Weiner, M.G., 2002. Visits to physicians after the oxygenation of gasoline in Philadelphia. *Archives of Environmental Health: An International Journal*, 57(2), pp.137-154.

Kampa, M. & Castanas, E., 2008. Human health effects of air pollution. *Environmental Pollution*, 151(2), pp.362–367.

Kan, H., Jia, J. & Chen, B., 2003. Acute stroke mortality and air pollution: new evidence from Shanghai, China. *Journal of occupational health*, 45(5), pp.321–323.

Khan, F.I. & Kr. Ghoshal, A., 2000. Removal of volatile organic compounds from polluted air. *Journal of Loss Prevention in the Process Industries*, 13(6), pp.527–545.

Klaas24.ee, 2017. Klaasi hinnad - Tavaline klaas. Available at: http://www.klaas24.ee/klaas.html [Accessed May 8, 2017].

Kolominsky, Y., Igumnov, S. & Drozdovitch, V., 1999. The psychological development of children from Belarus exposed in the prenatal period to radiation from the Chernobyl atomic power plant. *Journal of child psychology and psychiatry, and allied disciplines*, 40(2), pp.299–305.

Krýsa, J. et al., 2011. Effect of glass substrate and deposition technique on the properties of sol gel TiO_2 thin films. *Journal of Photochemistry & Photobiology, A: Chemistry*, 222(1), pp.81-86.

Lee, M.S., 2012. *Mass spectrometry handbook*, J. Wiley & Sons, p.946.

Li, W.B., Wang, J.X. & Gong, H., 2009. Catalytic combustion of VOCs on non-noble metal catalysts. *Catalysis Today*, 148(1–2), pp.81–87.

Lim, M. et al., 2009. Development and potential of new generation photocatalytic systems for air pollution abatement: an overview. *Asia-Pacific Journal of Chemical Engineering*, 4(4), pp.387–402.

Liu, S. et al., 2003. Association between gaseous ambient air pollutants and adverse pregnancy outcomes in Vancouver, Canada. *Environmental health perspectives*, 111(14), p.1773.

Lovett, G.M. et al., 2009. Effects of air pollution on ecosystems and biological diversity in the eastern United States. *Annals of the New York Academy of Sciences*, 1162(1), pp.99–135.

Lu, Y. et al., 2014. Feasibility analysis on photocatalytic removal of gaseous ozone in aircraft cabins. *Building and Environment*, 81, pp.42–50.

Mamaghani, A.H., Haghighat, F. & Lee, C.-S., 2017. Photocatalytic oxidation technology for indoor environment air purification: the state-of-the-art. *Applied Catalysis B: Environmental*, 203, pp.247–269.

Mo, J. et al., 2009. Photocatalytic purification of volatile organic compounds in indoor air: a literature review. *Atmospheric Environment*, 43, pp.2229–2246.

Mohammad, S., Mansooreh, S. & Reza, B., 2013. A brief review of methyl tert-butyl ether (MTBE) removal from contaminated air and water. *Research Journal of Chemistry and Environment Res.J.Chem.Environ*, 17(5), pp.90-97.

Moussavi, G. et al., 2009. Performance evaluation of a thermophilic biofilter for the removal of MTBE from waste air stream: effects of inlet concentration and EBRT. *Biochemical Engineering Journal*, 45(2), pp.152–156.

Nakajima, A. et al., 2005. Photocatalytic destruction of gaseous toluene by sulfated TiO_2 powder. *Catalysis Communications*, 6(11), pp.716–720.

Nakata, K. & Fujishima, A., 2012. TiO_2 photocatalysis: design and applications. *Journal of Photochemistry and Photobiology C: Photochemistry Reviews*, 13(3), pp.169–189.

National Science Foundation, 2017. Scanning Electron Microscopy (SEM). Available at: http://serc.carleton.edu/research_education/geochemsheets/techniques/SEM.html [Accessed April 30, 2017].

Nattero, G. & Enrico, A., 1996. Outdoor pollution and headache. *Headache: The Journal of Head and Face Pain*, 36(4), pp.243–245.

NCBI (National Center for Biotechnology Information), 2005. tert-Butyl methyl ether | $C_5H_{12}O$ - PubChem. Available at: https://pubchem.ncbi.nlm.nih.gov/compound/15413 [Accessed March 20, 2017].

NIOSH (The National Institute for Occupational Safety and Health), 2015. Methyl tert-butyl ether. Available at: https://www.cdc.gov/niosh/ipcsneng/neng1164.html [Accessed March 21, 2017].

Nishimura, A. et al., 2010. Using TiO_2 photocatalyst with adsorbent to oxidize carbon monoxide in rich hydrogen. *Catalysis Today*, 158(3), pp.296–304.

Novotná, P. et al., 2007. Two-component transparent TiO_2/SiO_2 and TiO_2/PDMS films as efficient photocatalysts for environmental cleaning. *Applied Catalysis B: Environmental*, 79(2), pp.179–185.

Ollis, D.F., 2000. Photocatalytic purification and remediation of contaminated air and water. *Comptes Rendus de l'Académie des Sciences - Series IIC - Chemistry*, 3(6), pp.405–411.

Pascal, M. et al., 2013. Assessing the public health impacts of urban air pollution in 25 European cities: Results of the Aphekom project. *Science of the Total Environment*, 449, pp.390–400.

PharmaXChange.info, 2011. Ultraviolet-Visible (UV-VIS) Spectroscopy – Principle. Available at: http://pharmaxchange.info/press/2011/12/ultraviolet-visible-uv-vis-spectroscopy-principle/ [Accessed April 30, 2017].

Pichat, P. et al., 2000. Purification/deodorization of indoor air and gaseous effluents by TiO_2 photocatalysis. *Catalysis Today*, 63(2), pp.363–369.

Power, M.C. et al., 2011. Traffic-related air pollution and cognitive function in a cohort of older men. *Environmental health perspectives*, 119(5), pp.682–687.

Preethi, T., Abarna, B. & Rajarajeswari, G.R., 2014. Influence of chitosan–PEG binary template on the crystallite characteristics of sol–gel synthesized mesoporous nano-titania photocatalyst. *Applied Surface Science*, 317, pp.90–97.

Ramírez-Santos, Á.A., Acevedo-Peña, P. & Córdoba, E.M., 2012. Enhanced photocatalytic activity of TiO_2 films by modification with polyethylene glycol. *Química Nova*, 35(10), pp.1931–1935.

Ren, H. et al., 2017. Photocatalytic materials and technologies for air purification. *Journal of Hazardous Materials*, 325, pp.340–366.

S.I. Howard Glass Co., 2013. Schott Borofloat Glass. Available at: http://flatglassproducts.howardglass.com/viewitems/flat-glass-products-fabrication/schott-borofloat-glass-2 [Accessed May 8, 2017].

Sakurai, K. & Mizusawa, M., 2010. X-ray diffraction imaging of anatase and rutile. *Analytical Chemistry*, 82(9), pp.3519–3522.

Schneider, J. et al., 2014. Understanding TiO_2 photocatalysis: mechanisms and materials. *Chemical Reviews*, 114(19), pp.9919–9986.

Sell, N.J., 1992. *Industrial pollution control: issues and techniques*, John Wiley & Sons, pp.239-240.

Sofuoglu, S.C. et al., 2010. An assessment of indoor air concentrations and health risks of volatile organic compounds in three primary schools. *International Journal of Hygiene and Environmental Health*, 214, pp.36–46.

Sonawane, R.., Kale, B.. & Dongare, M.., 2004. Preparation and photo-catalytic activity of Fe-TiO_2 thin films prepared by sol–gel dip coating. *Materials Chemistry and Physics*, 85(1), pp.52–57.

Soreanu, G., Dixon, M. & Darlington, A., 2013. Botanical biofiltration of indoor gaseous pollutants – a mini-review. *Chemical Engineering Journal*, 229, pp.585–594.

Spiridonova, J., 2016. Gas-phase photocatalytic reactor for the study of thin films' activity. *Digital Collection of Tallinn University of Technology Library*.

Stevens, L. et al., 1998. Investigation of the photocatalytic oxidation of low-level carbonyl compounds. *Journal of the Air & Waste Management Association*, 48(10), pp.979–984.

The Corning Museum of Glass, 2011. All About Glass | Types of Glass. Available at: http://www.cmog.org/article/types-glass [Accessed April 29, 2017].

UN Environment, Persistent organic pollutants (POPs) and pesticides. Available at: http://www.cep.unep.org/publications-and-resources/marine-and-coastal-issues-links/persistent-organic-pollutants-pops-and-pesticides [Accessed March 28, 2017].

US EPA, 2004. Technologies for treating MTBE and other fuel oxygenates. Available at: https://www.epa.gov/remedytech/technologies-treating-mtbe-and-other-fuel-oxygenates [Accessed March 20, 2017].

US EPA, 2016. Volatile organic compounds' impact on indoor air quality. Available at: https://www.epa.gov/indoor-air-quality-iaq/volatile-organic-compounds-impact-indoor-air-quality [Accessed March 28, 2017].

Vad, K., Csik, A. & Langer, G.A., 2009. Secondary neutral mass spectrometry - a powerful technique for quantitative elemental and depth profiling analyses of nanostructures. *Spectroscopy Europe*, 21(4), pp.13–16.

Verbruggen, S.W., 2015. TiO_2 photocatalysis for the degradation of pollutants in gas phase: from morphological design to plasmonic enhancement. *Journal of Photochemistry and Photobiology C: Photochemistry Reviews*, 24, pp.64–82.

Vohra, A. et al., 2006. Enhanced photocatalytic disinfection of indoor air. *Applied Catalysis B: Environmental*, 64(1–2), pp.57–65.

Wang, J.-D. et al., 1998. Occupational and environmental lead poisoning: case study of a battery recycling smelter in Taiwan. *Journal of toxicological sciences*, 23, pp.241–245.

Wang, Y. et al., 2000. The preparation, characterization, photoelectrochemical and photocatalytic properties of lanthanide metal-ion-doped TiO_2 nanoparticles. *Journal of Molecular Catalysis A: Chemical*, 151(1–2), pp.205–216.

Ware, J.H. et al., 1993. Respiratory and irritant health effects of ambient volatile organic compounds. *American Journal of Epidemiology*, 137(12), pp.1287–1301.

Wen, J. et al., 2015. Photocatalysis fundamentals and surface modification of TiO_2 nanomaterials. *Chinese Journal of Catalysis*, 36(12), pp.2049–2070.

WHO, 2014. Burden of disease from ambient and household air pollution for 2012. Available at: http://www.who.int/phe/health_topics/outdoorair/databases/FINAL_HAP_AAP_BoD_24March2014.pdf [Accessed March 20, 2017].

Wolkoff, P., 2013. Mini-Review Indoor air pollutants in office environments: assessment of comfort, health, and performance. *International Journal of Hygiene and Environmental Health*, 216, pp.371–394.

Xu, Y.-M., Yu, X.-H. & Liu, H.-J., 2002. Synthesis of TiO_2 Nanoparticles via a Ti(IV) complex with stearic acid and the photocatalytic activity for organic oxidation. *Chinese Journal of Chemistry*, 20(1), pp.9–13.

Yao, H. & Feilberg, A., 2015. Characterisation of photocatalytic degradation of odorous compounds associated with livestock facilities by means of PTR-MS. *Chemical Engineering Journal*, 277, pp.341–351.

Yoneyama, H. & Torimoto, T., 2000. Titanium dioxide/adsorbent hybrid photocatalysts for photodestruction of organic substances of dilute concentrations. *Catalysis Today*, 58(2), pp.133–140.

Yu, J. et al., 2000. Preparation, microstructure and photocatalytic activity of the porous TiO_2 anatase coating by sol-gel processing. *Journal of Sol-Gel Science and Technology*, 17(2), pp.163–171.

Zang, L. et al., 2000. Visible-light detoxification and charge generation by transition metal chloride modified titania. *Chemistry - A European Journal*, 6(2), pp.379–384.

Zeatoun, L. & Feke, D., 2005. Characterization of TiO_2 smoke prepared using gas-phase hydrolysis of $TiCl_4$. *Particle & Particle Systems Characterization*, 22(4), pp.276–281.

Zhang, T. et al., 2009. Antibacterial Behavior of Ag-Ce-TiO_2 composite films in the different irradiations. *Materials Science Forum*, 610–613, pp.463–466.

Zhao, J. & Yang, X., 2003. Photocatalytic oxidation for indoor air purification: a literature review. *Building and Environment*, 38, pp.645–654.

Zhao, Y. et al., 2009. Simultaneous SO_2 and NO removal from flue gas based on TiO_2 photocatalytic oxidation. *Environmental Technology*, 30(14), pp.1555–1563.

Zhao, Z. & Liu, Q., 2008. Effects of lanthanide doping on electronic structures and optical properties of anatase TiO_2 from density functional theory calculations. *Journal of Physics D: Applied Physics*, 41(8), p.085417.

Zhong, L. & Haghighat, F., 2014. Ozonation air purification technology in HVAC applications. Available at: https://www.researchgate.net/publication/260363850_Ozonation_Air_Purification_Technology_in_HVAC_Applications [Accessed March 22, 2017].

Zhong, L. & Haghighat, F., 2015. Photocatalytic air cleaners and materials technologies - abilities and limitations. *Building and Environment*, 91, pp.191–203.

Zita, J. et al., 2010. Photocatalytic properties of different TiO_2 thin films of various porosity and titania loading. *Catalysis Today*, 161, pp.29–34.

Zita, J., Maixner, J. & Krýsa, J.K., 2010. Multilayer TiO_2/SiO_2 thin sol–gel films: affect of calcination temperature and Na^+ diffusion. *Journal of Photochemistry and Photobiology A: Chemistry*, 216, pp.194–200.

Zogorski, J.S., Moran, M.J. & Hamilton, P.A., 2001. MTBE and other volatile organic compounds — new findings and implications on the quality of source waters used for drinking-water supplies. Available at: https://pubs.usgs.gov/fs/fs10501/pdf/fs10501.pdf [Accessed March 20, 2017].